UCSF
UC San Francisco Electronic Theses and Dissertations

Title
Age-Related Changes in Attentional Networks Underlie the Effects of Cognitive Aging

Permalink
https://escholarship.org/uc/item/0kj0c6fz

Author
Chadick, James Zachary

Publication Date
2010

Peer reviewed|Thesis/dissertation

eScholarship.org Powered by the California Digital Library
University of California

Age-Related Changes in Attentional Networks Underlie the Effects of Cognitive Aging

by

James Zachary Chadick

DISSERTATION

Submitted in partial satisfaction of the requirements for the degree of

DOCTOR OF PHILOSOPHY

in

Neuroscience

in the

GRADUATE DIVISION

of the

UNIVERSITY OF CALIFORNIA, SAN FRANCISCO

Copyright ©(2010)
by
James Zachary Chadick

Acknowledgements

For their support (science does not happened in a vacuum):

Leah McGuire, James and Kathleen Chadick, Gazzaley Lab members (past and present): Ted Zanto; Michael Rubens; Wes Clapp; Jon Kalkstein; Joaquin Anguera; Jean Rintoul; Jacqueline Boccanfuso; Anne Berry, Matt Paquette, Aaron Rutman, Judy Pa, Jacob Bollinger, Peter Wais, Jyoti Mishra Ramanathan, Nate Cashdollar, Jeff Cooney, Ezequiel Morsella, and Ian Greenhouse. Members of the NIC: Laura Stables, Paul Kesselman, and Vibhas Deshpande. Also thanks to Tim Verstynen, Jesse Rissman, Robert Sload, Bryan Smith, and Francisco Asturias.

Thesis Committee (for their mentoring and guidance):

- Adam Gazzaley – *Advisor: University of California, San Francisco*
- Loren Frank – *Thesis Chair: University of California, San Francisco*
- Christoph Schreiner – *University of California, San Francisco*
- Dan Mathalon – *University of California, San Francisco*
- Michael Silver – *Outside Member: University of California, Berkeley*

All work described below was conducted in the lab of and under the supervision of Professor Adam Gazzaley from Sept 2006 through November 2010.

Chapter 2 is currently in review at Nature Neuroscience in an abbreviated form. The coauthor listed in this publication (Adam Gazzaley) directed and supervised the research that forms the basis for the thesis.

Version 1.00
Typeset using LaTeX 2ε and BibTeX
Presented: November 29, 2010
Submitted: December 16, 2010

Abstract

Age-Related Changes in Attentional Networks Underlie the Effects of Cognitive Aging

James Zachary Chadick

The initial stages of age-related cognitive decline manifest themselves through fairly innocuous, fleeting moments of everyday life: moments of forgetfulness, reduced ability to multitask, and an increased susceptibility to distraction. However, as we age, these symptoms become progressively worse and potentially debilitating. What began as innocently as going to the refrigerator only to have forgotten the item we wished to retrieve can quickly progress to events that have serious health and societal consequences. As the global population is rapidly aging, this problem takes on particular urgency. In the studies below, we set out to examine the age-related inability to successful allocate attentional resources, in particular we were concerned with the global neural networks that may drive these processes, how they change with age, how they influence behavior, and if there is a neuro-structural underpinning for this decline. In effect, we wanted to know why and how does the brain age.

In our first experiment, we set out to determine how the brain allocates attentional resources and what neural networks are involved. We utilized a selective attention,

working memory paradigm while recording whole-brain neural activity using functional magnetic resonance imaging (fMRI) in healthy, young controls. We found evidence that there exist separate neural networks associated with the attentional processes of enhancement (increasing the neural response to task-relevant information) and suppression (decreasing the neural response to task-irrelevant stimuli) of visual cortices. Specifically, we found that neural enhancement was associated with the frontal-parietal network (a network thought to be associated with the process of orienting attention to external stimuli) and suppression was associated with the default network (a network thought to be associated with various *internal* cognitive processes such as introspection and mind-wandering). Interestingly, the frontal-parietal network is traditionally associated with allocation of attention while the default network is suppressed during attentionally demanding tasks. These network activity changes co-vary with the effects of neural enhancement and suppression within the visual cortex (Chapter 2).

The finding that two separate networks are involved in enhancement and suppression presented an attractive target for studying age-related functional and cognitive changes. It has been shown that 1) older adults have deficits in suppression of irrelevant information compared to younger participants, i.e. an age-related selective suppression deficit and 2) there is an age-related dysfunction in the default network. Thus, since the results above suggest a link between suppression and the default network, our hypothesis was that we would find corresponding age-related changes in a healthy, older population. Indeed, this was the case; older participants showed a reduced ability to suppress task-irrelevant information and exhibited a corresponding reduction in default network function. Most significantly, however, we found that gray-matter atrophy within a node of the default network (the medial prefrontal cortex, mPFC) was correlated with declines in both suppression and cognitive performance (Chapter 3). These findings support our hypothesis that age-related neuro-structural changes underlie the selective suppression deficit

and, more generally, the effects of cognitive aging.

Contents

Abstract iv

1 Introduction 1

2 Attention Networks in Healthy, Youngs 8

2.1 Abstract . . . 8

2.2 Introduction . . . 9

2.3 Results . . . 12

2.3.1 Behavioral Performance . . . 12

2.3.2 Univariate data for stimulus-selective, visual association cortex areas . . . 13

2.3.3 Whole-Brain functional connectivity . . . 15

2.3.4 Direct Comparison of the Suppression Network and Enhancement Network . . . 19

2.3.5 Comparison of the Suppression Network and the Default Network . . . 20

2.3.6 Suppression Network vs. Visual Cortical Activity Suppression 21

2.3.7 Reaction-time data vs. Whole-brain activity . . . 22

2.3.8 Relationshp between RT and VAC connectivity . . . 22

2.4 Discussion . . . 23

2.5 Materials and Methods . . . 27

2.5.1 Participants . . . 27

2.5.2 Experimental Design . . . 27

2.5.3 Stimuli . . . 29
2.5.4 Localizer and Default Network . . . 29
2.5.5 fMRI Collection and Processing . . . 30
2.5.6 Network Analysis . . . 31
2.5.7 Whole-Brain Neural-Functional Connectivity Correlations . 32
2.5.8 Whole-Brain Reaction Time Correlations with Activity . . . 32
2.5.9 Whole-Brain Behavioral-Functional Connectivity Correlations 33
2.5.10 Comparative Statistics . . . 33

3 Age-Related Neuro-functional Changes 40

3.1 Abstract . . . 40
3.2 Introduction . . . 41
3.3 Results . . . 44
3.3.1 Behavioral . . . 44
3.3.2 Univariate ROI Results . . . 47
3.3.3 Relationship Between Behavioral Performance and Suppression 50
3.3.4 Relationship between Gray-Matter Atrophy and WM Performance . . . 52
3.3.5 Relationship between Gray-Matter Atrophy and Neural Suppression . . . 53
3.3.6 Age-Related Changes to the Suppression Network . . . 54
3.3.7 Age-Related Alterations to the Default Network . . . 56
3.3.8 Default Network Deactivation and Age-Related Neural and Behavioral Changes . . . 57
3.4 Discussion . . . 58
3.4.1 Behavioral Analysis . . . 59
3.4.2 Age-Related Selective Suppression Deficit . . . 60
3.4.3 mPFC Atrophy, WM and Suppression Impairment . . . 61
3.4.4 Age-Related Changes to the Suppression Network . . . 62

3.4.5 Age-Related Changes to the Default Network 63
3.5 Conclusion 63
3.6 Materials and Methods 64
3.6.1 Participants 64
3.6.2 Neuropsychological Testing 64
3.6.3 Experimental Design 65
3.6.4 Stimuli 67
3.6.5 Localizer and Default Network 67
3.6.6 fMRI Collection and Processing 68
3.6.7 VBM Analysis 69
3.6.8 Network Analysis 69
3.6.9 Whole-Brain Neural-Functional Connectivity Correlations . 70
3.6.10 Comparative Statistics 70

4 Conclusions **71**

A Aging Enhancement Changes **76**
A.1 Introduction 76
A.2 Results and Discussion 78

Appendices **76**

B rTMS Effects **81**
B.1 Introduction 81
B.2 Materials and Methods 82
B.3 Results and Discussion 84

Literature Cited **89**

List of Figures

2.1 Experimental Paradigm 13

2.2 Behavioral Results 14

2.3 Encoding Period Activity for Visual Association Cortex Regions of Interest 15

2.4 Network Connectivity 17

2.5 Default and Suppression Networks 35

2.6 Default Network ROIs 36

2.7 mPFC Coupling with VAC 37

2.8 Suppression and mPFC Coupling 37

2.9 Trial-by-Trial Correlation Between RT and Whole-Brain Activity . 38

2.10 Correlation Between Distraction and RT 39

3.1 Experimental Paradigm 45

3.2 Behavioral Results 46

3.3 Univariate VAC ROI Results 48

3.4 PPA Enhancement and Suppression Indices 50

3.5 Neural-Behavioral Correlations 52

3.6 Voxel Based Morphometry Results 53

3.7 Younger vs. Older Suppression Network 55

3.8 Younger vs. Older Default Network 57

3.9 Relationship Between Default Network Suppression and Performance 58

A.1 Younger vs. Older Enhancement Network 79

B.1 rTMS Task 83
B.2 Behavioral Performance 84
B.3 PPA ROI Results 85
B.4 Univariate Activity Effects of rTMS 86
B.5 RT-MFG Activity Correlation 86
B.6 rTMS Effects on Attentional Networks 87
B.7 rTMS Effects on PPA Connectivity 88

List of Tables

2.1 Enhancement Network 18
2.2 Suppression Network 19
2.3 Comparison of Enhancement and Suppression 34

Chapter 1

Introduction

> *When I was younger, I could remember anything, whether it had happened or not; but my faculties are decaying now and soon I shall be so I cannot remember any but the things that never happened. It is sad to go to pieces like this but we all have to do it . . .*
>
> *-Mark Twain*

As we age, we suffer a progressive decline in cognitive abilities [1, 2]. There is a gradual, age-related decline in working memory performance and capacity on selective attention tasks as well as overall reductions in executive function. In addition, there are significant neuro-structural and functional changes [3] associated with the aging process such as increased gray matter atrophy (particularly within the prefrontal cortex, PFC) [4] and decreased white matter organization (i.e. increases in white-matter hyper-intensities and degradation of long-range cortico-cortico fiber tracks) correlated with cognitive decline [1, 3, 5, 6]. One prominent manifestation of age-related cognitive decline is the inability to ignore task-irrelevant, or distracting information [7, 3]. Given the reduced neural capacity of older adults [8], a failure to ignore irrelevant information is, in effect, a misallocation of attentional resources that results in an age-related decline in selective-attention working memory performance [9]. Our hypothesis is that older adults show neuro-structural deficits

consistent with age-related cognitive declines and that these underlying structural changes are the root cause of older adults inability to ignore task-irrelevant information [3].

Goal-directed, or top-down, modulation is what allows us to successfully navigate multiple competing, simultaneous sensory demands [10, 11]. When external stimuli are relevant to the task at hand, we show a corresponding increase, or enhancement, in neural activity within regions selective for these stimuli; when stimuli are irrelevant, these same regions show a decrease, or suppression, of neural activity [12, 13]. It is this top-down modulation that serves as the foundation for successful working memory performance [14]. However, as we age, there is a specific decline in our ability to suppress task-irrelevant information. This age-related selective suppression deficit is coupled to working memory performance, where those older adults who show the greatest suppression are those who show the best working memory performance [3]. It is unclear as to why this neural deficit is selective for suppression but we hypothesize that underlying changes to the attentional networks associated with suppression are the root cause. In this model of cognitive aging, there are age-related declines specific to the suppression network – perhaps due to underlying age-related neuro-structural changes – that manifest themselves as a selective suppression deficit.

The ability to modulate visual cortical regions based on attentional goals is not an intrinsic local property of these areas but instead results from the action of distributed neural networks involving the prefrontal, parietal, and visual lobes [15]. Reciprocal cortico-cortico white matter tracks have been observed using tract-tracing studies [16, 17, 18, 19] and are thought to underlie this top-down modulation. Additionally, lesion studies in both primates and humans [20, 21, 22, 23, 24], transcranial magnetic stimulation (TMS) [25], and functional connectivity [15] have demonstrated that perturbation in distal brain regions affects goal-driven modulation of visual regions. Therefore, age-related disruptions of distal brain regions

involved in top-down modulation (such as the PFC) can result in decreased modulatory ability and the corresponding behavioral decline [3].

Two attention-related whole-brain networks have recently been described and are tempting to link with the processes of enhancement and suppression due to their divergent response in the face of attentionally demanding tasks. The frontal-parietal network shows an increased level of activation, or enhancement, in response to attention tasks [26, 27] while the default network shows decreased neural activity, or suppression, in response to attentionally demanding tasks [28, 27, 29], mirroring the results observed in visual regions in response to task-relevant or task-irrelevant stimuli. Interestingly, the default network is associated with various *internal* cognitive processes such as prospective memory and mind wandering [30, 31]. Since both of these internal processes can be thought of as internally-generated distractions, providing a link between suppression and the default network would suggest that this network is important in mediating both internal and external distractors.

Additionally, demonstrating a link between the default network and the process of suppression would provide a potential mechanism for the age-related inability to suppress task-irrelevant information. In older adults, there is a severe disruption in default network function [1, 28]. Older adults show a decreased ability to suppress the default network during attentionally demanding tasks [32] and decreased network fidelity where regions such as the mPFC become decoupled from the default network [33, 34]. Our hypothesis is that these age-related changes to the default network underlie the age-related selective suppression deficit, although the causality of this statement cannot be addressed using observation techniques such as fMRI alone.

In the experiments below, we utilized a selective-attention, working memory task while recording whole-brain neural activity using functional magnetic resonance imaging (fMRI). In this task, participants simultaneously viewed images containing both task-relevant and task-irrelevant stimuli superimposed to minimize spatial

attention effects [13]. We were able to extract visual associative cortex (VAC) regions that were selective to one or the other of our two stimuli (faces and scenes) and were able to extract neural measures of top-down modulation (i.e. enhancement and suppression) [12]. In addition, our whole-brain recording technique allowed us to sample distal brain regions during the task and extract the neural networks differentially associated with the processes of enhancement and suppression [15].

In Chapter 2, we looked at the whole-brain networks associated with the processes of enhancement and suppression in healthy, young controls. Task-instructions showed a clear effect on regions of the VAC depending on whether the encoded stimulus was task-relevant or task-irrelevant. When VAC regions encoded a task-relevant stimulus, there was an enhancement of the neural response compared to baseline, while in the task-irrelevant case, there was a suppression of the neural response, as has been described previously [12]. When we extracted the whole-brain networks associated with enhancement and suppression, we found a novel result. Instead of enhancement and suppression being associated with similar whole-brain networks, we found that task-relevant VAC regions were functionally coupled with the frontal-parietal network while task-irrelevant VAC regions were functionally coupled with the default network. It was unsurprising that we found the frontal-parietal network associated with enhancement as this network is traditionally described as a large-scale brain network that is co-activated by attentionally demanding tasks. Since the process of enhancement is simply the neural response to directing attention to a task-relevant stimulus, this qualifies as an attentionally demanding task and has previously been reported as functionally connected to visual regions [35, 26].

Novel was the coupling between suppression and the default network. Previous studies have described the default network in one of two ways: 1) regions that are correlated in time in the absence of external, attentionally demanding tasks [1, 27] or 2) regions whose activity is suppressed during attentionally demanding tasks

[32]. It is thought that default network activity is reflective of internal cognitive processes such as prospective memory and mind wandering [28, 27, 29] that must be suppressed for successful attention allocation to external goals. It is logical that these regions of the default network were the same regions associated with the suppression network. In this framework, the suppression of task-irrelevant, externally generated stimuli is intimately linked with the suppression of task-irrelevant, internally generated distractions.

Notably, we found that the relationship between the default network and task-irrelevant VAC regions was maintained only in the presence of distracting information and that this coupling is independent of stimulus type. For both VAC regions used in our analysis, we observed a simultaneous coupling between task-relevant regions and the frontal-parietal network and between task-irrelevant regions and the default network that switches based on task goals and independent of VAC region used. Furthermore, our results indicated that both suppression of the default network and maintenance of the VAC-default network coupling in the task-irrelevant conditions was key to successful behavioral performance. This supports the theory that successful suppression of task-irrelevant information is the driving force behind working memory performance in divided attention tasks and that in populations that exhibit decreased suppression (such as older adults, 60+ years old), there is a corresponding decrease in performance [3].

Chapter 3 directly examined the age-related declines in neural function and structure and their role in cognitive aging. Using the paradigm and differential enhancement and suppression networks described for the healthy, young controls above, we ran the same selective attention, working memory paradigm in healthy older participants. Given that older adults show a demonstrable age-related selective suppression deficit [3], our hypothesis was that we would find an altered suppression network in healthy older adults consistent with their inability to suppress task-irrelevant information. In addition, we hoped to decipher the age-related

neuro-structural underpinnings of this dysfunction. When we extracted enhancement and suppression networks in older adults, we found a severe disruption in their suppression network where regions that were functionally involved in healthy, young controls (such as the medial prefrontal cortex, mPFC) were no longer associated with suppression of task-irrelevant VAC regions consistent with the older adults' suppression deficit [3].

Since the mPFC is a prominent node within the default network [27], we also investigated measures of default network function (namely attentionally demanding task-induced deactivations) and their relationship in age-related neural and cognitive deficits. We found that older adults who maintained suppression, were best able to maintain performance on our task. In addition, we found that those participants who had greatest default network function (as measured by task-induced deactivations), were the same participants who maintained both neural markers of suppression and behavioral performance compared to healthy, young controls. Taken together, these results suggest that as we age, default network function degrades resulting in an inability to neurally suppress task-irrelevant stimuli (whether internally i.e. mind wandering or externally generated), which results in an inability to successfully perform attentionally demanding tasks.

Notably, however, we were also able to link this behavioral and neural decline in older adults to underlying structural changes. We found that gray matter atrophy within the mPFC is highly predictive of both participants' ability to suppress task-irrelevant information and their decline in working memory performance. Older participants who showed the greatest atrophy within the mPFC also showed the greatest selective suppression deficit and decline in working memory performance. These results buttress our hypothesis that default/suppression network dysfunction is a principal driving force behind age-related cognitive decline.

The studies described in the above two chapters paint an attractive theoretical underpinning for one of the prominent effects of cognitive aging, specifically the age-

related inability to ignore task-irrelevant information. In this model, age-related gray-matter atrophy within the mPFC disrupts participants' default network and suppression network. This disruption results in an inability to neurally suppress task-irrelevant information and a corresponding reduction in performance. Thus the age-related selective suppression deficit may play a large role in age-related cognitive decline [3, 2] and likely has a genesis in underlying age-related structural changes.

Chapter 2

Differential Coupling of Visual Cortical Areas with the Default Network or Frontal-Parietal Network Based on Task Goals

2.1 Abstract

Recent studies describe distinct whole-brain functional networks whose component regions are differentially enhanced or suppressed depending on cognitive state. It has been demonstrated that focusing attention on goal-relevant information while ignoring irrelevant information involves differential enhancement and suppression of sensory cortical activity. However, the relationship between goal-driven, or top-down, modulation in sensory cortices and activity in distributed brain regions comprising large-scale networks remains unclear. Connectivity analysis of functional magnetic resonance imaging data showed visual cortical areas processing relevant information were functionally connected with the dorsal frontal-parietal

network, while visual areas processing irrelevant information were simultaneously coupled with the default network. Importantly, we show the strength of visual cortex/default network functional connectivity was predictive of participants' abilities to suppress irrelevant information. This provides the first evidence that sensory cortical regions are dynamically coupled with distinct neural networks based on goals, suggesting differential involvement of these networks in top-down enhancement and suppression.

2.2 Introduction

Goal-directed decisions influence our perception of stimuli and result in corresponding modulation of sensory cortical activity. This phenomenon, known as top-down modulation, is characterized by increased cortical responses when stimuli are task-relevant (i.e., enhancement) and decreased responses when stimuli are task-irrelevant (i.e., suppression) [12, 10, 36]. It is this modulatory ability that allows us to successfully interact in complex environments and navigate multiple streams of sensory information in a flexible, dynamic manner, thus serving as a foundation for higher-order cognitive processes, such as working memory (WM) and long-term memory [13, 14].

Top-down modulation during visual processing is not thought to be an intrinsic property of visual cortices, but rather achieved via distributed connections between brain regions, or neural networks, notably involving the prefrontal cortex (PFC), parietal cortex (PC) and the visual association cortex (VAC) [15]. The reciprocal cortico-cortical connections between PFC, PC and VAC found in animal tract-tracing studies provide a structural basis for this interaction [16, 17, 18, 19]. Functionally, the network model of top-down modulation is supported by converging evidence from studies involving brain lesions and physiological recordings in both animals and humans [20, 21, 22, 24], as well as transcranial magnetic

stimulation [25] and human fMRI studies utilizing functional connectivity analysis [15].

It remains to be proven whether enhancement and suppression are mechanistically distinct processes or exist as a continuum of the same underlying mechanism. Recent evidence suggests that enhancement and suppression are independent processes. For example, they are differentially impacted by aging [3, 37] and cognitive load manipulations [38], suggesting that they may be associated with distinct neural networks. However, a recent fMRI study revealed that networks involved in enhancement and suppression are very similar, though the strength of PFC-VAC coupling correlates with the magnitude of attentional enhancement and suppression of VAC activity [15]. Notably, the Gazzaley et al. (2007) study utilized sequential stimuli presentation and thus did not generate direct competition for visual processing resources. The biased competition model of top-down modulation proposes that suppression of irrelevant information is driven via competition amongst multiple stimuli for limited visual processing resources [39]. Thus, distinguishing networks involved in top-down enhancement and suppression may require simultaneously competing visual demands. To address this, the current study utilized images with superimposed relevant and irrelevant visual information [13].

In recent years, there has been an accumulation of studies directed at exploring how large-scale brain networks are involved in goal-directed behavior and in non goal-directed activities, such as when participants are passive at rest. Two networks that have generated extensive interest are the frontal-parietal network (or dorsal attention network) [26, 27] and the default network [28, 27, 29]. The frontal-parietal network includes regions in the PFC, inferior frontal junction (IFJ), supplementary motor area (SMA), and superior intraparietal sulcus (sIPS) [27] and is co-activated during a wide-array of goal-directed tasks, including selective attention, [35, 40] visual search [41] and WM [15]. The brain regions in the default network are a distinct network: the medial prefrontal cortex (mPFC); medial, lateral, and in-

ferior parietal cortex (mPC, lPC, and iPC); retrosplenial cortex (ReSp); and the precuneus/posterior cingulate cortex (PCC) [42] and was first described as a set of regions that were de-activated during goal-directed behavior [29]. However, the default network has been further implicated as an ensemble of regions functionally connected at rest that are activated during introspective cognitive functions, such as prospective and retrospective memory and internal monitoring [30, 31]. Thus, in a manner that parallels top-down activity modulation in sensory cortices, distinct sets of parietal and frontal regions exhibit enhanced and suppressed activity dependent on the cognitive state of the individual. To our knowledge, the relationship of activity fluctuations in these large-scale networks with top-down enhancement and suppression of sensory cortices has not been explored.

The goal of this study was to evaluate networks associated with top-down modulation in the setting of simultaneous, competing visual processing demands, so as to place enhancement and suppression networks in the context of recently established large-scale brain networks. We utilized fMRI during a selective WM task in which participants were required to remember task-relevant stimuli, while simultaneously ignoring distracting stimuli (i.e., superimposed faces and natural scenes) [13]. Because bottom-up (or stimulus-driven) information was constant across conditions, brain regions functionally connected to modulated, sensory cortical areas reflect networks associated with enhancement or suppression driven by task requirements. Functional connectivity maps were generated by differentially pairing conditions with stimulus-selective visual cortical regions that, with respect to task goals (e.g., "attend to faces"), selectively represented relevant (e.g., the face) and irrelevant aspects of the stimulus (e.g., the scene) [15]. By contrasting these networks with functional connectivity maps during a passive viewing task, we identified distinct enhancement and suppression networks.

2.3 Results

2.3.1 Behavioral Performance

WM accuracy and response time (RT) data were subjected to separate repeated-measures 2x2 analysis of variance (ANOVA) with type of stimuli attended (face vs. scene) and overlap status (overlapped vs. non-overlapped) as factors (Fig. 2.1). WM accuracy analysis revealed a main effect of overlap ($F_{1,21} = 70.1$; $p < 0.0001$), such that accuracy was significantly reduced in tasks with overlapped stimuli relative to tasks with face and scene stimuli presented in isolation (Face-Memory-Overlap: FM-O – 79.4% vs. Face-Memory: FM – 88.6%, $p < 5x10^{-7}$; Scene-Memory-Overlap: SM-O – 78.3% vs. Scene-Memory: SM – 92.6%, $p < 1x10^{-12}$) (Fig. 2.2A). This WM performance reduction for the overlapping stimuli was also evident as an increased RT for the overlap tasks ($F_{1,21} = 28.4$; $p < 0.0001$), (FM-O – 1323 ms vs. FM – 1197 ms, p ¡ 0.002; SM-O – 1144 ms vs. SM – 1303 ms, $p < 0.001$) (Fig 2.2B). This supports previous findings that overlapped stimuli involve conflicting information that reduces WM performance [13]. There was also a main effect of type of stimulus attended for WM accuracy ($F_{1,21} = 4.8$; $p < 0.05$), but no interaction between stimulus type and overlap ($F_{1,21} = 1.17$; $p < 0.287$). Post-hoc comparisons revealed that accuracy was reduced for faces compared to scenes, but only in the non-overlapped tasks (SM – 92.6%, FM – 88.6%, $p < 0.01$). There was no main effect of stimulus for RT, and no interaction between stimulus and overlap for RT. Accuracy in the passive view (PV-O) task was 99.1%; reaction times to arrow direction averaged 697 ms.

In addition to measures of WM performance, participants also performed a post-experiment evaluation of long-term memory (Fig. 2.2C). Participants had higher long-term retention of stimuli from the non-overlapped conditions (FM and SM) compared to the overlapped conditions (FM-O, SM-O, and PV-O, $p < 0.005$).

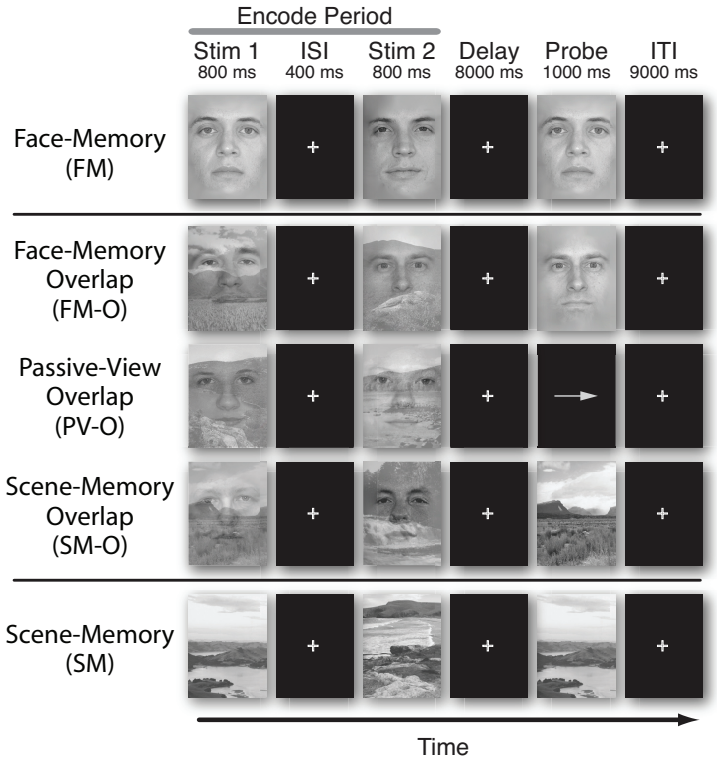

Figure 2.1: *Experimental Paradigm.* Participants were instructed to remember Stim1 and Stim2 and respond yes/no if the probe image matched either of the previous two stimuli. Participants maintained fixation on the white crosshairs throughout experiment.

In addition, for overlapped stimuli, participants remembered task-relevant stimuli significantly better than task-irrelevant stimuli (e.g., faces in the FM-O > scenes in FM-O, $p < 0.05$).

2.3.2 Univariate data for stimulus-selective, visual association cortex areas

Neural measures of top-down modulation in visual cortices were derived by modeling encoding-period activity using a GLM and extracting β-values (activation maps) associated with activations from the left PPA and right FFA , as previous studies show these are the most robust regions of face and scene selective activity modulation [15, 12, 38]. Data from the PPA revealed the expected bottom-up

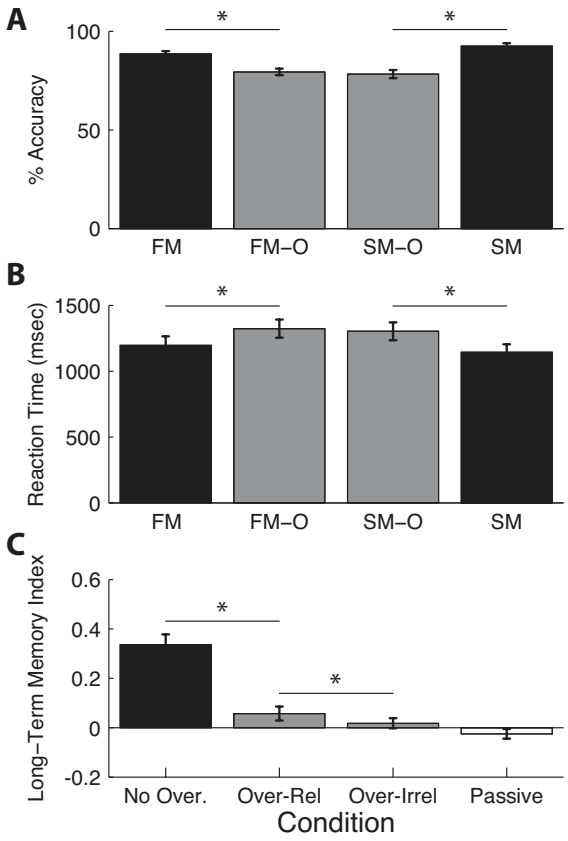

Figure 2.2: *Behavioral Results.* A. Accuracy comparisons for participants across all conditions (n=22). There is an effect of performance on overlapped images (FM-O and SM-O) compared to non-overlapped images (FM and SM), but no effect of stimulus type (FM-O vs. SM-O and FM vs. SM). B. Reaction-time comparisons. Similar results as in A. C. Long-term memory scores. Participants remembered stimuli with no overlap significantly better than those with overlap ($p < 0.005$). In the overlapped conditions, task-relevant images were retained better than task-irrelevant images ($p < 0.05$). Black colors represent no distractor, grey – distractors, white – passive-view. Error-bars represent S.E.M.

scene-selectivity of this region, such that stimuli that include scenes alone (SM) demonstrated significantly greater responses than stimuli with faces alone (FM) (Fig. 2.3A). In addition, there was a significant top-down modulation effect, such that all three overlapped conditions revealed significantly different patterns of activation depending on the goals of the task: enhancement of PPA activity when scenes were relevant compared to passive-view baseline (SM-O > PV-O; $p < 0.001$), and significant suppression of PPA activity when scenes were irrelevant compared to baseline (FM-O < PV-O; $p < 0.005$), consistent with the ROI results using a

similar paradigm with sequential presentation of faces and scenes [12]. These three levels of activation (SM-O > PV-O > FM-O) represent a pure, top-down effect because bottom-up information was constant across tasks. In addition, the magnitude of the ROI effects for the overlapped conditions fell between the levels attained in pure conditions (SM > SM-O > PV-O > FM-O > FM). A similar pattern of activation was observed for the FFA (Fig. 2.3B). A significant bottom-up effect was demonstrated, such that FM > SM, as well as significant enhancement (FM-O > PV-O). However, there was not a robust measure of suppression within the FFA (SM-O < PV-O), consistent with a previous finding investigating enhancement and suppression within the VAC [12] yet the FFA did exhibit overall top-down modulation where FM-O > SM-O.

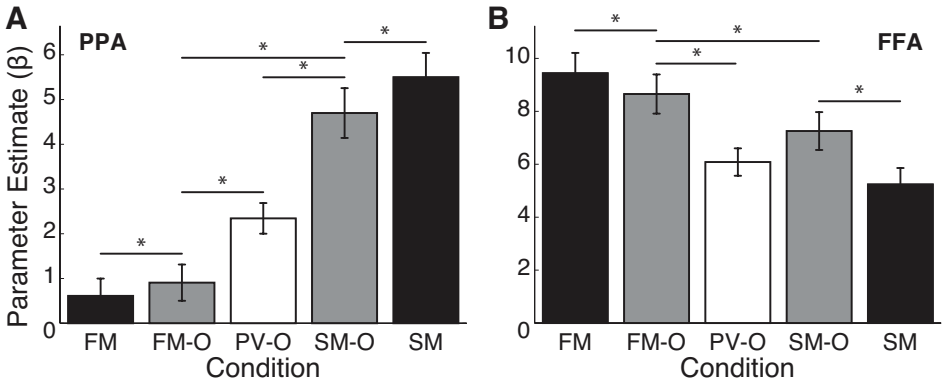

Figure 2.3: *Encoding period activity for visual association cortex regions of interest.* Parameter estimates for a scene-selective region (parahippocampal place area: PPA) are significantly different between each condition, with the difference between SM-O and PV-O reflecting enhancement and the difference between PV-O and FM-O reflecting suppression. B. Same as A, but using the face-selective region (face fusiform area: FFA) ($*p < 0.05$). Error-bars represent S.E.M.

2.3.3 Whole-Brain functional connectivity

Capitalizing on trial-by-trial variability, whole-brain functional connectivity maps were assessed by correlating activity from the VAC ROIs (seed regions) with voxels from the rest of the brain [43, 44]. Regions that are highly correlated with a

VAC seed across trials are presumed to be functionally connected, thereby defining large-scale networks associated with activity modulation that occurs in those regions. By differentially pairing a seed with a task condition, enhancement and suppression networks can be evaluated. An *enhancement network* map was generated by contrasting PPA connectivity maps obtained during SM-O with those during PV-O (i.e., comparing the PPA network map during the condition when scenes were behaviorally relevant, to the network from the condition when there were no attentional demands. Note: the same stimuli and seed regions were used, just the pairing of seed and condition differed) [15]. Comparably, a *suppression network* map was generated by contrasting the PPA connectivity maps obtained in the FM-O and PV-O contrast (i.e., comparing the condition when scenes were behaviorally irrelevant, to the condition when there were no attentional demands). Brain regions more strongly correlated with the PPA in SM-O and FM-O compared to PV-O are potentially associated with enhancement and suppression processes, respectively. The same analysis was performed using the FFA as a seed region and differentially pairing it with conditions to yield enhancement and suppression networks. Note that these analyses are correlational and do not reveal that enhancement and suppression network regions are sources of top-down control, but rather that they are associated with VAC regions that are enhanced or suppressed. Interestingly, even though the FFA does not show a robust measure of suppression (Fig. 2.3B), the FFA shows a top-down effect where relevant-stimuli activity (i.e. FM-O) is significantly greater than irrelevant-stimuli activity (i.e. SM-O). This observed coupling between the FFA and the putative *suppression network* may assist in driving this overall modulation.

Analysis of the whole-brain enhancement networks demonstrated that visual cortical ROIs representing relevant information were functionally connected with regions that have been previously defined as the frontal-parietal network (FPN) [26, 27]: the right middle frontal gyrus (MFG), bilateral inferior frontal junction (IFJ,)

superior intraparietal sulcus (sIPS), and supplementary motor area (SMA) (Fig. 2.4A & B, Table 2.1). Interestingly, the enhancement network using the PPA seed (Fig. 2.4A) involved similar regions as the enhancement network using the FFA seed (Fig. 2.4B). This suggests that comparable frontal and parietal regions are associated with enhancement of task-relevant visual stimuli regardless of stimulus type, consistent with these regions being involved in a diverse array of attentionally demanding tasks [45, 26, 15, 41].

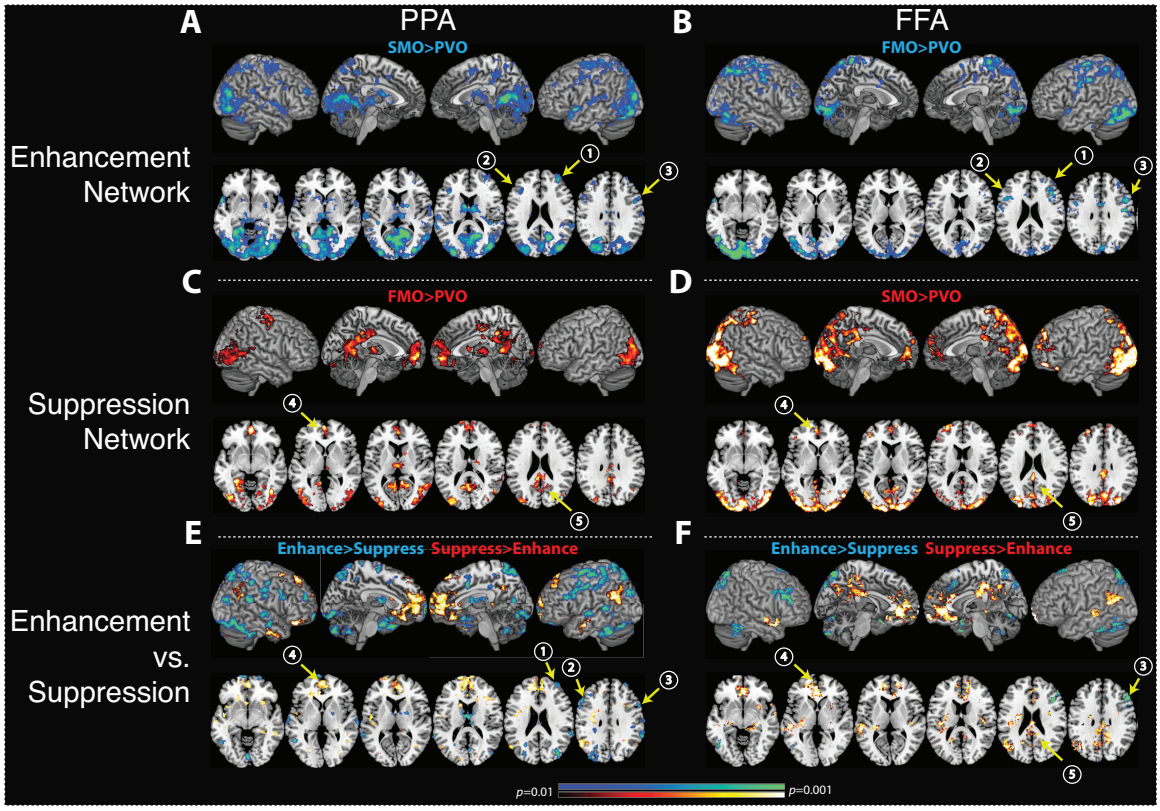

Figure 2.4: *Network Connectivity.* Connectivity Maps associated with enhancement (A and B, SM-O>PV-O and FM-O>PV-O, respectively), suppression (C and D, FM-O>PV-O and SM-O>PV-O, respectively), and contrast maps between suppression and enhancement networks (E and F) for both PPA (A, C, and E) and FFA (B, D, and F). Whole-brain maps were cluster corrected for multiple comparisons at p=0.05 and displayed at $p < 0.01$. Labeled regions are as follows: 1) right MFG, 2) left IFJ, 3) right IFJ, 4) mPFC, and 5) PCC.

Analysis of the suppression network revealed a different set of regions from those identified in the enhancement network. Specifically, regions in the medial prefrontal cortex (mPFC), posterior cingulate cortex (PCC), retrosplenial cortex (ReSp), and

bilateral parietal cortex (PC) were functionally coupled with visual cortical seeds representing the irrelevant stimuli (Fig. 2.4C & D, Table 2.2). Notably, these brain regions are key nodes of the default network (DN) [28, 27]. As with the enhancement network, the suppression network was observed to be largely independent of seed region (PPA – Fig. 2.4C and FFA – Fig. 2.4D), despite the FFA not achieving significant suppression (yet, showing significant overall top-down modulation).

Table 2.1: *Enhancement Network.* Regions that exhibit significantly greater functional connectivity for Remember > Passively View for scenes (PPA: SMO > PVO) and faces (FFA: FMO > PVO). Significance was determined as described in methods: whole-brain images were thresholded at $p < 0.05$ using FDR and cluster correction. Coordinates are in MNI space.

PPA Enhancement (SM-O > PV-O)

NAME	X	Y	Z
right Middle Frontal Gyrus (rMFG)	34	44	36
left Middle Frontal Gyrus (lMFG)	48	12	34
left Inferior Frontal Junction (lIFJ)	-48	2	32
right Inferior Frontal Junction (rIFJ)	50	2-	24
Supplementary Motor Area (SMA)	2	2	58
right Superior Parietal Lobule (rSPL)	30	-58	56

FFA Enhancement (FM-O > PV-O)

NAME	X	Y	Z
right Middle Frontal Gyrus (rMFG)	38	44	36
right Inferior Frontal Junction (rIFJ)	48	12	34
left Inferior Frontal Junction (lIFJ)	-48	2	32
Supplementary Motor Area (SMA)	0	2	46
right Frontal Eye Fields (rFEF)	48	-12	48
left Frontal Eye Fields (lFEF)	-46	-12	46
right Superior Parietal Lobule (rSPL)	44	-48	56
left Superior Parietal Lobule (lSPL)	-40	-48	54

Table 2.2: *Suppression Network.* Regions that exhibit significantly greater functional connectivity for the Ignore > Passively view for scenes (PPA: FMO > PVO) and faces (FFA: SMO > PVO). Significance was determined as in Table 2.1. Coordinates are in MNI space.

PPA Suppression (FM-O > PV-O)

NAME	X	Y	Z
medial Prefrontal Cortex (mPFC)	2	56	-6
Posterior Cingulate Cortex (PCC)	2	-40	34
Retrospinial Cortex (reSp)	-4	-58	16
right Angular Gyrus (rAngG)	40	-64	40

FFA Suppression (SM-O > PV-O)

NAME	X	Y	Z
medial Prefrontal Cortex (mPFC)	-4	52	2
left Frontal Pole (lFP)	-32	50	30
left Middle Frontal Gyrus (lMFG)	-42	42	10
Posterior Cingulate Cortex (PCC)	0	-34	32
left Superior Parietal Lobule (lSPL)	24	-64	60

2.3.4 Direct Comparison of the Suppression Network and Enhancement Network

To evaluate which regions were unique to the enhancement or suppression networks, we directly contrasted the enhancement and suppression networks (Fig. 2.4E & F, Table 2.3). This analysis revealed distinct networks and highlighted regions specific to the enhancement network, notably the right MFG, left IFJ, and right IFJ (Fig. 2.2E & F: blue colors; labeled 1, 2, and 3, respectively), and regions specific to the suppression network, notably DN regions such as the mPFC and PCC (Fig. 2.4E & F: red colors; labeled 4, and 5, respectively), as well as a large region of the left lateral parietal cortex.

2.3.5 Comparison of the Suppression Network and the Default Network

To explore the relationship between the suppression network and the DN, a whole-brain conjunction analysis was performed in which voxels were identified that showed both significant suppression network connectivity and DN activity corrected for cluster size (Fig. 2.5). The suppression networks were assessed using both PPA and FFA seeds. The DN was identified using the independent localizer task and contrasting rest > task blocks (Fig. 2.5A and B, first rows), which yielded the canonical DN [28, 27]. Strikingly, the conjunction analysis revealed that there was a high degree of overlap between the suppression networks and the medial regions of the DN, most notably the PCC and mPFC. (Fig. 2.5A and B, bottom rows (magenta)).

We further explored this relationship by using DN ROIs identified by the independent localizer. Consistent with our previous observations, we demonstrated greater functional connectivity between visual cortical regions and DN regions when the information represented by stimulus-selective visual regions was irrelevant to the participant's goals, compared to when the information was relevant (notably, mPFC, and PCC) (Fig. 2.6). For example, the PPA exhibited greater connectivity with mPFC and PCC during the condition when scenes were irrelevant (FM-O), than the condition when scenes were relevant (SM-O). This pattern was consistent for the same stimuli using a different seed region, such that the FFA demonstrated greater connectivity with the mPFC and PCC in the condition when scenes were irrelevant (SM-O), than the condition when faces were relevant (FM-O). Moreover, analysis revealed that differential connectivity of stimulus-selective visual regions with DN regions occurred simultaneously, such that differential connectivity was present during each condition. For example, during FM-O, there was greater connectivity between the mPFC and PPA than with FFA, a pattern that was reversed

with the same stimuli but when task goals were switched (i.e., during SM-O, there was greater connectivity between the mPFC and FFA than with PPA) (Fig. 2.7, middle panels). Interestingly, this phenomenon required the presence of irrelevant information. In conditions without task-irrelevant information present (i.e., FM and SM), but with the same goals as when stimuli contained irrelevant information (i.e., FM-O and SM-O), neither the PPA nor the FFA were significantly connected with DN regions (Fig. 2.7, outer panels). Thus, the suppression network depicted in Fig. 2.4C and D are generated based on task goals, but requires the presence of conflicting, irrelevant information.

Because of the correlational nature of the network measure, there is the possibility that the DN/VAC relationship may not exist in the non-overlap condition because of less signal variance in the contributing regions. Analysis of the standard deviation of the BOLD signal across trials within each participant and then evaluated at the group level revealed that neither the mPFC nor the PPA showed significant differences in the unitless $r-$value variance between the overlapped (FM-O) and non-overlapped (FM) conditions (mPFC: 0.7605 and 1.0142, respectively: t-test, $p = 0.5$; PPA: 1.7510 and 1.8433, respectively: t-test, $p = 0.8$). This suggests that the lack of coupling in the non-overlapped conditions compared to the overlapped condition is evidence that the relationship between DN and sensory regions reflects a more complex interaction, one dependent on the presence of irrelevant information.

2.3.6 Suppression Network vs. Visual Cortical Activity Suppression

To further explore the relationship between VAC activity modulation and network connectivity, we performed across-participant, whole-brain regression analyses. While we did not find connectivity with any FPN regions that served as

significant predictors of the magnitude of activity enhancement, the magnitude of PPA suppression was predicted by the degree of functional connectivity between the PPA and the mPFC (Fig. 2.8), such that participants with stronger coupling between the PPA and mPFC showed greater suppression of activity associated with task-irrelevant scenes. This effect was limited to PPA, consistent with the univariate ROI results that revealed PPA exhibited more robust suppression than FFA (Fig. 2.3).

2.3.7 Reaction-time data vs. Whole-brain activity

We performed a regression analysis of trial-by-trial response times (RTs) and BOLD signal across every voxel in the brain for each participant. On the group level, we demonstrated that trial-by-trial activity fluctuations within DN regions were significantly correlated with RT (particularly the mPFC and PCC; corrected for multiple comparisons) in the overlapped conditions, such that trials that exhibited the greatest suppression of activity in DN regions during stimulus presentation were those trials that exhibited the fastest RT at probe (high performance) (Fig. 2.9A). When the RT-activity correlation was performed on those conditions without overlapping stimuli, there was no significant correlation (Fig. 2.9B). When overlapped vs. non-overlapped correlations were directly compared, we demonstrate that the correlation was significantly greater in the overlapped vs. non-overlapped conditions (Fig. 2.9C). This neural-behavioral finding is comparable to the results showing that significant DN coupling with visual areas occurs only when task-irrelevant stimuli are present.

2.3.8 Relationshp between RT and VAC connectivity

We performed an across-participant regression analysis between the impact of irrelevant information on behavioral performance (RT for overlapped condition minus

RT for non-overlap condition (FM-O minus FM)) and the impact of irrelevant information on functional coupling between the PPA and the rest of the brain (FM-O minus FM). This demonstrated a strong and significant negative correlation between RT and PPA-mPFC functional connectivity, a component of the DN (corrected for multiple comparisons). These data revealed that those participants who exhibited stronger coupling between mPFC and PPA when task-irrelevant information was present, versus when it was absent (i.e., larger difference between FM-O and FM), better preserved their performance when irrelevant information was present, compared to when it was absent (i.e., smaller difference between FM-O and FM) (Fig. 2.10). Of note, this same relationship was not significant when the FFA was the seed region and SM-O and SM were the conditions, consistent with the lack of significant suppression in the FFA.

2.4 Discussion

The data presented provide the first direct evidence that sensory cortex is differentially associated with defined functional networks based on task goals. When visual cortex is associated with behaviorally relevant stimuli (i.e. they are to be actively remembered), we demonstrated both that visual cortex shows an increased neural response to the stimuli relative to a passive viewing condition (enhancement) and that it is functionally correlated with activity in the FPN. Conversely, when sensory input is to be actively ignored, sensory cortex (specifically, the PPA) shows a decreased neural response relative to passive viewing (suppression) and is functionally coupled with the DN. Interestingly, both these modulatory/network-association processes occur simultaneously and switch based on task goals, independent of stimulus type. These results present a novel association between sensory cortex and putative frontal and parietal top-down control regions.

The enhancement network corresponds closely to a network shown to be associ-

ated with attentional and executive processes. This network, largely revealed via univariate analysis, has been referred to by various terms, including the FPN, dorsal-attention network and the task-positive network [28, 27, 46, 40], although the general set of regions is consistent across naming schemes. A proposed role of these dorsal frontal and parietal regions is that they are the source of top-down modulatory influences on sensory cortical activity, such that they provide direct, long-range signaling to sensory areas to enhance activity based on task goals [35]. This is supported by functional neurophysiological studies in experimental animals [23, 47, 24]. Our interpretation of the robust functional connectivity between enhanced VAC regions and this network is that these areas are sources of top-down control (Table 2.1). This conclusion is also supported by our previous study using fMRI connectivity analysis and sequential, rather than simultaneous stimulus presentation [15].

It is important to note that fMRI approaches are correlational in nature and are unable to be used to make strong statements of causality. Another approach would be to utilize a recording technique with high temporal resolution (such as EEG) to investigate the timing of distal communication (for example, do both the FPN and the DN act in an anticipatory fashion prior to stimulus onset as a mechanism for "priming" VAC regions based on task-goals or is there real-time communication that allows efficient processing of stimuli within selective VAC regions). However, EEG is also correlational and so to truly establish causality in demonstrating that area A is communicating with area B, the system would have to be carefully perturbed in a controlled fashion using a technique such as transcranial magnetic stimulation, and coupled with a recording technique. Since our results indicate that separate networks are differentially involved in the processes of enhancement and suppression, one could perturb a node differentially involved in either enhancement or suppression to prove causality by showing that you selectively disrupt the neural signature of enhancement or suppression.

Suppression of activity within DN regions has been observed during goal-directed behavior [48, 33, 46, 34, 32]. Here we extend these findings by showing that trial-by-trial fluctuations in activity within DN regions, notably the mPFC, covaries with activity fluctuations of VAC representing irrelevant, external information. Given the overlap between the suppression network and the DN (Fig. 2.5), it is reasonable to speculate that DN regions are a direct source of VAC activity suppression. However, if DN regions were truly a source of suppressive influence, one might expect there to be a negative correlation. That is, if on a given trial VAC activity was reduced, then activity in frontal and parietal regions of the suppression network serving as the source of such modulation might be expected to be elevated. Instead we find a positive correlation, such that reduced VAC activity is linked with lower activity in DN regions.

Recent evidence suggests that the DN is related to introspective or internalized cognitive processes, such as mind-wandering [30, 31], and retrospective and prospective memory [28, 31]. Activity in DN regions, notably the mPFC [49], are increased during these internal processes [30, 50, 31], while they are suppressed during tasks that are directed at external events [48, 33, 46, 34, 32], presumably as a means of reducing internal distraction. In fact, the degree of deactivation and fidelity of this collective network is predictive of performance [1, 33]. Based on this literature, our interpretion of the overlap between the suppression network and the DN is that it reflects a coupling across trials of suppression of irrelevant external information and suppression of internal activities, both of which if not suppressed would conflict with achieving the goals of the task. This link suggests that a common mode of suppression of task-irrelevant information is engaged regardless if our internal or external environment presents a conflict with task goals. One of the most intriguing aspects of our results is that the degree of activity suppression in the PPA correlated with the degree of connectivity between the PPA and the mPFC during the act of scene suppression. This implies that there may be a facilitatory aspect

of the coupling between these two acts of suppression. In addition, there was a significant relationship between the degree of coupling and WM performance across participants.

The finding in this study of functional connectivity between the suppression network and DN is in direct contrast to results reported previously using a sequential presentation version of this task, which revealed a topographically overlapping FPN for enhancement and suppression, with reduced connectivity during suppression [15]. It is possible that the disparity may reflect differences in the demands of the two tasks, since DN deactivation has been shown to be modulated by cognitive load [51], such that increased load results in greater deactivation. However, since the results were not quantitatively, but qualitatively different, it raises interesting questions regarding the nature of conflict and the neural systems utilized when resolving conflict. In the current study, there was direct competition for visual processing recourses, while in the sequential version of the task the competition was indirect, and presumably between new information and information maintained in WM. The combined data suggest that ignoring irrelevant information encountered in isolation involves diminished connectivity between visual regions and FPN, while when irrelevant information is in direct conflict with ongoing sensory processing it involves coupling visual regions (in this case, the PPA) with the DN. In support of this finding, the results of the current study revealed that the coupling of suppressed VAC regions and the DN only existed in the presence of conflicting task-irrelevant information.

The overlap between the suppression network and the DN may elucidate findings that normal aging is associated with both a deficit in suppressing external irrelevant information [7, 3, 37] and a decreased ability to deactivate the DN during tasks [28, 33, 46, 52, 34]. This may represent further evidence of a relationship between these networks and a possible mechanistic basis to account for age-related suppression deficits. Functional imaging studies in older adults will be important in examining

the relationship between suppression of distraction from both the internal and external environment.

2.5 Materials and Methods

2.5.1 Participants

Functional and high-resolution anatomical MRI images were obtained from 22 healthy young participants (ages: 18-34, mean: 23.7) while performing the task described below. Participants were recruited and compensated monetarily as per the UCSF Committee on Human Research (CHR) approval. All participants had normal or corrected-to-normal vision and were taking no psychotropic medications. One participant was excluded from all analysis due to excessive motion artifacts ($>$ 3 mm) within the scanner.

2.5.2 Experimental Design

The experimental paradigm comprised five similar tasks in a delayed recognition working memory (WM) task design (Fig. 2.1), similar to previously published work [13]. Each task consisted of the same basic temporal sequence with only the instructions differing across tasks. All tasks involved viewing two images (Stim1, Stim2), each displayed for 800 ms (with a 400 ms inter-stimulus interval [ISI]) followed by a 8 second period (Delay) in which the images were to be remembered and mentally rehearsed. After the delay, a third image appeared (Probe) for 1000 sec. The participant was instructed to respond with a button press (as quickly as possible without sacrificing accuracy) whether or not the Probe image matched either of the previous two images (Stim1 or Stim2). This was followed by an inter-trial interval (ITI) lasting 9 seconds.

For three of the five tasks, the Stim1 and Stim2 images were composed of both a scene and a face superimposed upon each other. Participants were instructed to focus their attention on and remember either the face or the scene, while ignoring the other. In the face memory-overlap task (FM-O), the faces were remembered while the scenes were ignored, and vice versa in the scene memory-overlap task (SM-O). When the Probe image appeared, it was composed of an isolated face in the FM-O task, and an isolated scene in the SM-O task. For the passive view (PV-O) task, participants were instructed to view the overlapped images without trying to remember them, after which they responded to an arrow direction with a button press. For the other two tasks, the Stim1 and Stim2 images were composed of a single stimulus without any distracting/overlapping information: a face in the face memory task (FM) and a scene in the scene memory task (SM). The task was presented in 2 separate blocks, each block consisting of all 5 task sets counterbalanced in random order across all participants. Each task set consisted of 30 trials (60 total trials per task, 120 total Encode Period images).

Following the main experiment, participants performed a surprise post-experiment recognition test in which they viewed 320 non-overlapped images, including 160 faces and 160 scenes. 80 of the faces and 80 of the scenes were novel stimuli that were not included in the main experiment. There were 20 faces each from the FM, FM-O, SM-O, and PV-O tasks, and 20 scenes each from the SM, SM-O, FM-O, and PV-O tasks. No stimuli in the post-experiment test were seen more than once before. All included face and scene stimuli (both novel images and images from the experiment) were randomly ordered, and participants were asked to rate their recognition of each image on a scale from 1 – 4. For analysis of these data, each participant's ratings were collapsed across stimulus type and normalized to their average rating for novel stimuli. Scores were then collapsed across conditions and broken into the following categories: No-Overlap (stimuli from the SM and FM conditions), Overlap-Relevant (scenes and faces from the SM-O and FM-O

conditions, respectively), Overlap-Irrelevant (faces and scenes from the SM-O and FM-O conditions, respectively), and Passive-View (faces and scenes from the PV-O condition).

2.5.3 Stimuli

All stimuli consist of 225x300 pixel grayscale images, presented foveally, subtending a visual angle of 3° from a small cross at the center of the image. The face stimuli consisted of a variety of neutral-expression male and female faces across a large age range. Hair and ears were removed digitally, and a blur was applied along the contours of the face as to remove any potential non-face-specific cues. The gender of the face stimuli was held constant within each trial. Images of scenes were not digitally modified beyond resizing and grayscaling. For the tasks consisting of overlapped faces and scenes, one face and one scene were randomly paired, made transparent, and digitally overlapped using Adobe Photoshop CS2 such that both were equally visible. Overlapped and isolated images were randomly assigned to the different tasks.

2.5.4 Localizer and Default Network

To identify visual association cortex (VAC) regions maximally responsive to scenes and faces (the parahippocampal place area – or PPA – and the fusiform face area – or FFA), a localizer task independent of the main experimental task was performed, which consisted of 14 interleaved, 12 sec blocks of 20 scenes or faces with a 8 sec delay between each block [3, 12]. To ensure participant's maintained vigilance, they were asked to press a button whenever they saw the exact same stimulus presented twice in a row (10% of stimuli presented). fMRI data were acquired and processed as described below. A contrast was created from the general linear model (GLM) -maps for scenes and faces and the most active 35 voxels ($\backsim$0.390 cm^3) were se-

lected from the approximate anatomical location for each of the following: left PPA (lPPA), right PPA (rPPA), left FFA (lFFA), and right FFA (rFFA) [12]. Default network activity was functionally defined as regions where there was greater degree of activity during rest compared to 1-back [46]. ROIs for the default network were defined using clusters of activity anatomically constrained to published coordinates of network nodes [27].[1]

2.5.5 fMRI Collection and Processing

All fMRI data were collected on a Siemens 3T MAGNETOM Treo 3T scanner with stimuli presented on an LCD monitor viewed in the prone position by participants using a mirror rigidly attached to the 12-channel head-coil. Echoplanar imaging (EPI) data was acquired ($FA = 90°$, $T_E = 25$ ms, $T_R = 2$ sec) with 33 interleaved axial slices (with a 0.5 mm gap) for a final resolution of 1.79x1.79x3.5mm/voxel ($FOV = 23$ cm; 128x128 matrix). All data preprocessing was conducted in SPM5 (Wellcome Department of Imaging Neuroscience, London, England). Raw blood oxygen level dependent (BOLD) data were corrected offline for slice-timing acquisition and motion-artifacts. A 5mm isotropic Gaussian smoothing kernel was applied using SPM5 prior to modeling the data. In addition to the EPI data, high-resolution T1-MPRAGE images (1x1x1 mm voxel size; FOV = 160 x 240 x 256 mm, $T_R = 2300$ ms, $T_E = 3$ ms, $FA = 90°$) were acquired to aid in anatomical localizations of activity and to screen for any undiagnosed neurological trauma.

Region of interest (ROI) activities were calculated by modeling the encoding (including both stimuli and the ISI), delay periods, and probe periods in each condition using a boxcar function convolved with the canonical hemodynamic response function (HRF) for the duration of each epoch as a general linear model (GLM)

[1] It should be noted, that the default network was generated via univariate analysis, which technically does not reveal a "network". However, the same set of default regions have also been shown via functional connectivity analysis during a period of a rest [30]

within SPM5. Native-space masks for each posterior ROI were created for each participant as described above and the estimated coefficients for encode-period activity were used as a measure of posterior VAC activations. Group-level univariate analysis was performed by normalizing each participant's mean EPI image to the Montreal Neurological Institute (MNI; 2x2x2 mm voxel size) template image prior to Gaussian smoothing and modeling.

2.5.6 Network Analysis

Functional connectivity network maps were created for each participant as described previously using a β-series correlation analysis approach [43, 44]. The encode, delay and probe stage from each condition and every trial was modeled with its own distinct regressor within the GLM, although only the encode period activity was analyzed below. The average value was extracted for each VAC ROI for each trial and these values were then correlated voxel-wise across the entire brain to find regions with co-varying activity across trials with the VAC-ROI. The whole-brain r value maps for each participant underwent a Fisher's r to z transformation and the z-maps were then normalized to the MNI-template and Gaussian smoothed (5 mm FWHM) for group level analysis. Group contrast maps were created by permuting across the condition grouping term and averaging across the group using 10000 rounds of permutation [53]. Data were corrected for multiple comparisons by thresholding the p-values at 0.05 and permuting across the expected cluster distribution to find the expected cluster size for $p = 0.05$. Clusters smaller than this value were removed from the analysis [53].

2.5.7 Whole-Brain Neural-Functional Connectivity Correlations

Correlations between each participant's index of suppression (encode period values for the PPA: the difference between the FM-O and PV-O conditions) and the degree of functional connectivity between the PPA and every other voxel were performed on MNI-normalized images, thresholded at $p < 0.05$ and corrected for multiple comparisons using the permutation method described in the Network Analysis section above.

2.5.8 Whole-Brain Reaction Time Correlations with Activity

Using the β-series approach as described above, RT data were correlated with trial-by-trial variations in the modeled BOLD signal for every voxel in the brain for each participant. A Fisher's r to z transformation was applied and followed by t-tests to determine regions exhibiting significant correlations at the group level independently for both the main-effects of the overlapped condition (FM-O) and the non-overlapping condition (FM). To determine which regions were correlated significantly different between the overlapped and non-overlapped conditions, a contrast of z-values was created (FM-O – FM) and significance was determined using 10000 rounds of a permutation test (described above). Both main-effects and contrast images were thresholded at $p < 0.05$ and corrected for multiple comparisons using the permutation method described in the Network Analysis section above.

2.5.9 Whole-Brain Behavioral-Functional Connectivity Correlations

A behavioral index was created for each participant using the difference in RTs for the overlapped condition (FM-O) and the non-overlapped condition (FM) to normalize participants' performance by bottom-up sensory processing. Each participant's behavioral index was correlated on a voxel-by-voxel basis with a functional connectivity index composed of the difference in PPA connectivity in the overlapped (FM-O) and non-overlapped conditions (FM) [13]. This analysis was performed on MNI-normalized images, thresholded at $p < 0.05$ and corrected for multiple comparisons using the permutation method described in the Network Analysis section above. This same analysis was also performed using the FFA as a seed regions and SM-O and SM as the conditions.

2.5.10 Comparative Statistics

ANOVA's were utilized throughout analysis. Post-hoc two-tailed t-tests were corrected for multiple comparisons using Tukey-Kramer's method.

Table 2.3: *Comparison of Enhancement and Suppression.* Regions significantly different in a contrast between enhancement and suppression network maps. Significance was determined as in Table 2.1. Coordinates are in MNI space.

PPA Enhancement > Suppression

NAME	X	Y	Z
right Middle Frontal Gyrus (rMFG) 34	54	26	
right Inferior Frontal Junction (rIFJ)	54	12	38
left Inferior Frontal Junction (lIFJ)	-56	12	34
Supplementary Motor Area (SMA)	-4	12	46
right Intraparietal Sulcus (rIPS)	36	-44	42
right Angular Gyrus (rAngG)	36	-76	24
left Inferior Parietal Lobule (lIPL)	-38	-84	34

FFA Enhancement > Suppression

NAME	X	Y	Z
right Inferrior Frontal Junction (rIFJ)	40	8	38
right Middle Frontal Gyrus (rMFG)	50	28	32
Supplementary Motor Area (SMA)	0	16	66
right Superior Parietal Lobule (rSPL)	16	-72	60
left Superior Parietal Lobule (lSPL) -12	-72	58	

PPA Suppression > Enhancement

NAME	X	Y	Z
medial Prefrontal Cortex (mPFC)	2	52	0
right Frontal Pole (rFP)	42	38	-16
right Insula (rIN)	44	4	-12
left Insula (lIN)	-42	6	-16
left Superior Frontal Gyrus (rSFG)	-22	30	40
left Inferior Parietal Lobule (lIPL)	-50	-56	36
Posterior Cingulate Cortex (PCC)	6	-52	34
Retrospinial Cortex	-4	-58	16
right Inferior Temporal Cortex (rITC)	54	-10	-26

FFA Suppression > Enhancement

NAME	X	Y	Z
medial Prefrontal Cortex (mPFC)	-4	52	2
left Frontal Pole (lFP)	-32	50	30
left Temporalparietal Junction (lTPJ)	-54	-32	4
Posterior Cingulate Cortex (PCC)	0	-34	32
left Inferior Parietal Lobule (lIPL)	-48	-68	26

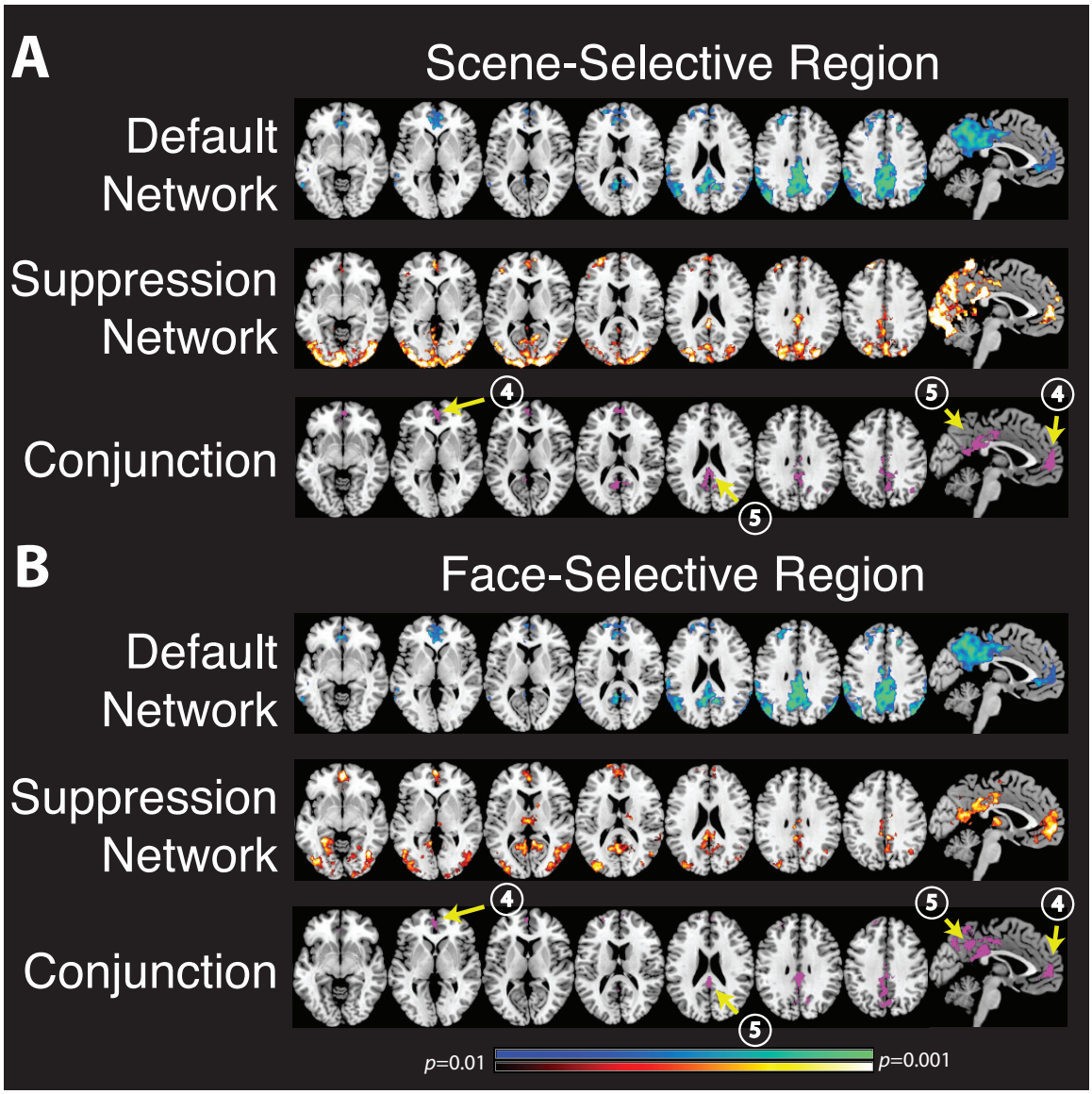

Figure 2.5: *Default and Suppression Networks.* Comparisons between the default-network and suppression network for PPA (A) and FFA (B). Whole-brain maps were cluster corrected for multiple comparisons at $p = 0.05$ and displayed at $p = 0.01$. Note that the first row in both A and B are the same images and are only repeated to allow ease of visual comparisons. Same numbered labels as in Figure 2.4.

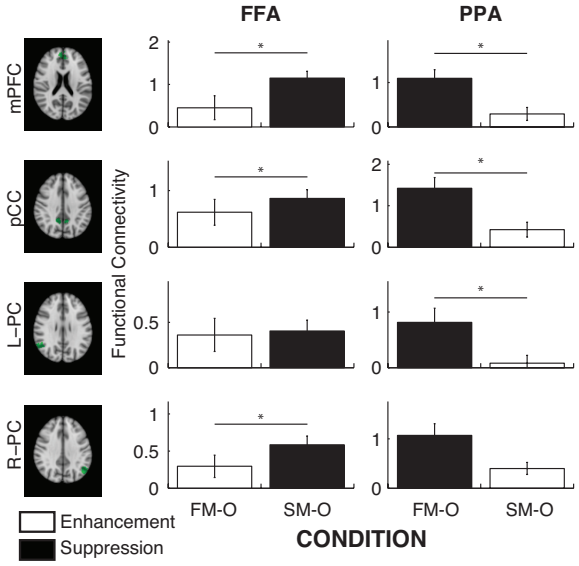

Figure 2.6: *Default Network ROIs.* Extracted functional connectivity data for visual association cortex (FFA and PPA) – default-network regions of interest, comparing between the remember faces (FM-O) and remember scenes (SM-O) conditions. White bars represent connectivity values during enhancement and black bars during suppression ($*p < 0.05$). Error-bars represent S.E.M.

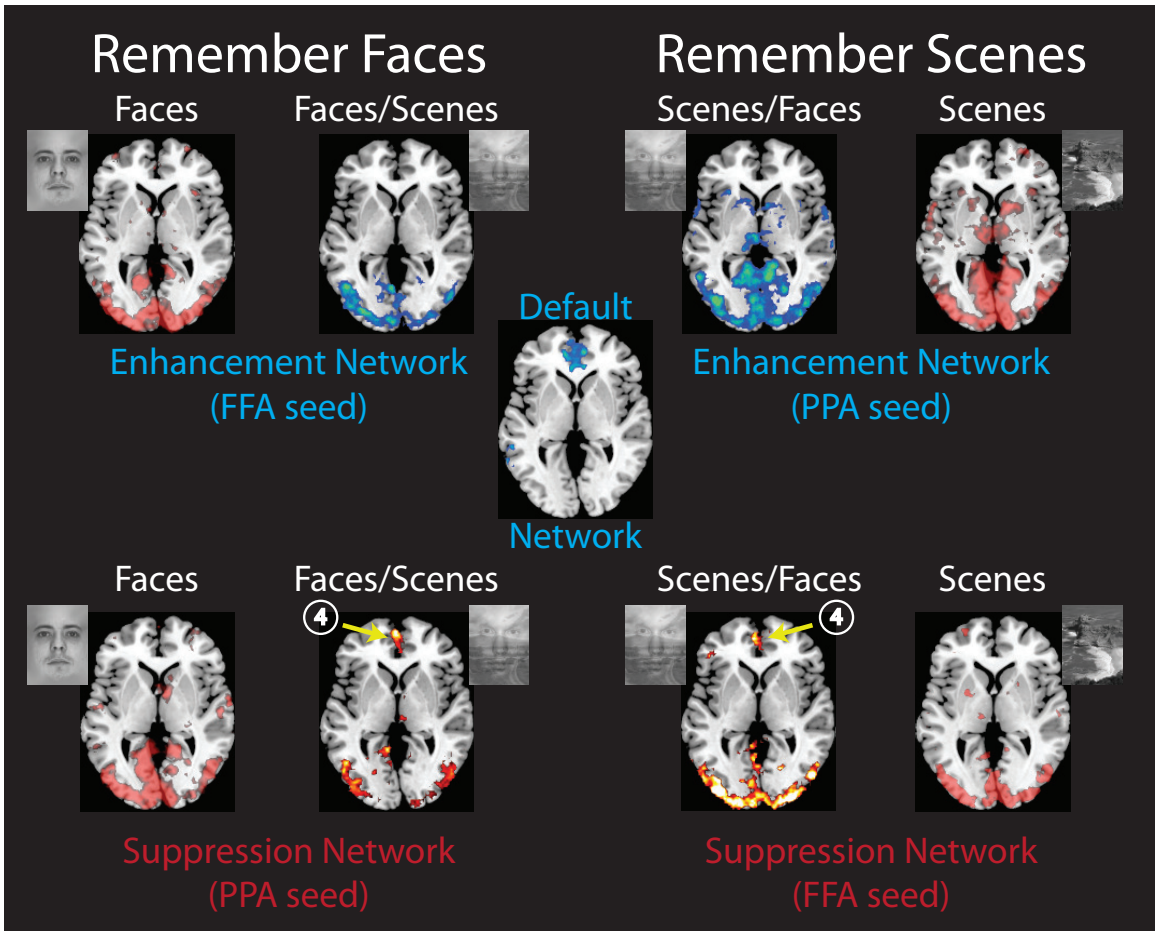

Figure 2.7: *mPFC Coupling with VAC.* Functional connectivity maps focusing on mPFC connectivity with different VAC seeds across conditions. Inner panels, upper vs. lower reveals selective connectivity of VAC regions and mPFC only in the suppression network. However, this mPFC connectivity only occurs when irrelevant information is present in the image (compare outer panels). Same numbered labels as in Figure 2.4.

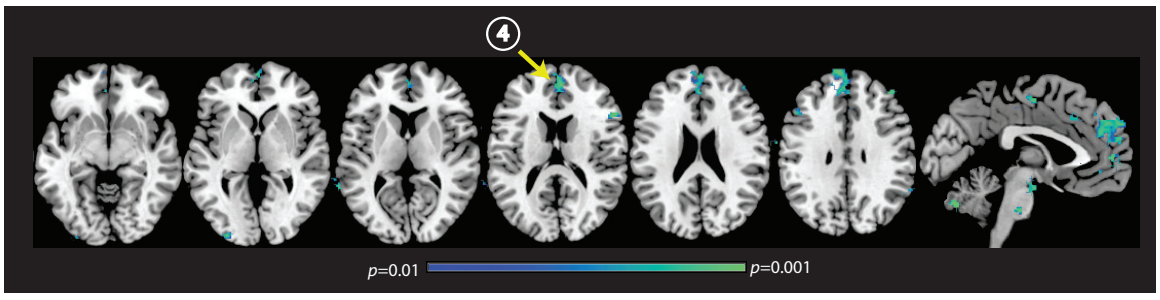

Figure 2.8: *Suppression and mPFC Coupling.* Group-data of a voxel-wise regression between the magnitude of PPA suppression (i.e. the PPA activity associated with PV-O – FM-O) and PPA functional connectivity (i.e the PPA connectivity values at every voxel, evaluated as: FM-O – PV-O) showing a significant correlation in the mPFC ($p < 0.05$ for Pearson's correlation corrected for multiple comparisons, see methods). Same numbered labels as in Fig. 2.4.

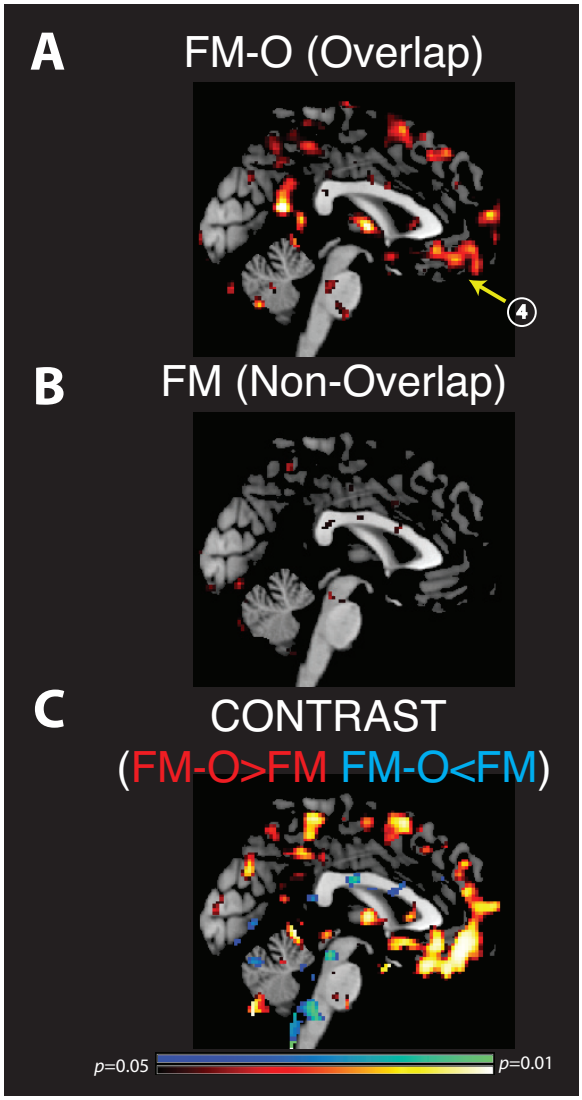

Figure 2.9: *Trial-by-Trial Correlation Between RT and Whole-Brain Activity.* A. Whole-brain correlation between RT data and activity during the FM-O condition. B. Whole-brain correlation between RT data and activity during the FM condition (non-overlapped images, no irrelevant information present). C. Contrast of A vs. B showing that activity in default mode regions was only correlated with RT when task-irrelevant information was present. Images displayed at $p < 0.05$ with cluster correction. Same numbered labels as in Figure 2.4.

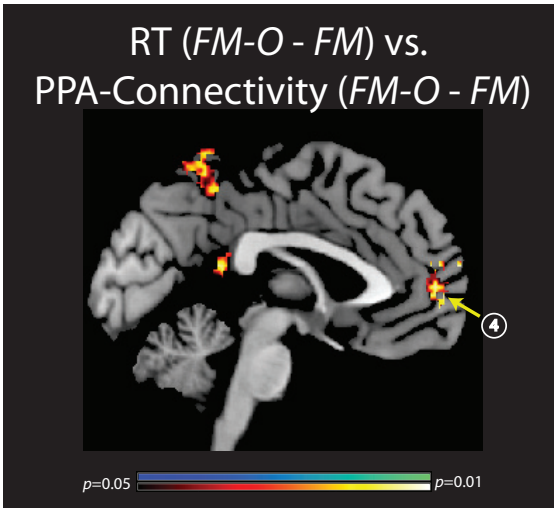

Figure 2.10: *Correlation Between Distraction and RT.* Whole-brain correlation between the impact of distraction on RT (FM-O – FM) and the impact of distraction on functional connectivity with the VAC (FM-O – FM). There was a strong negative correlation (red) between DN-PPA connectivity and the RT measure suggesting that greater VAC-DN functional connectivity is associated with better behavioral performance the setting of distracting information. No significant positive correlations (blue) were observed ($p < 0.05$). Same numbered labels as in Figure 2.4.

Chapter 3

Age-Related Changes to the Default Network Underlie the Suppression Deficit and Working Memory Impairment in Older Adults

3.1 Abstract

Older adults have long been known to exhibit age-related cognitive decline in areas such as executive function and working memory (WM). However, the exact mechanisms that underlie this decline have not been explored. Recent evidence from electroencephalography (EEG) and functional magnetic resonance imaging (fMRI) studies suggests that WM performance decline is related to an inability to ignore task-irrelevant – or distracting – information and that whole-brain networks, such as the default network are associated with successful suppression of irrelevant

information. To test the hypothesis that anatomical and functional changes to whole-brain networks, particularly the default network, underlie working memory impairment in older adults, fMRI was performed on both older and younger participants while they had to simultaneously attend to task-relevant visual stimuli while ignoring spatially overlapping distracting stimuli. Analysis revealed that WM performance is impaired by disruptions to the default network in healthy, older adults consistent with both WM and suppression deficits previously described. These results support the hypothesis that default network function is key to successful suppression of irrelevant information and that changes to this network may underlie the effects of cognitive aging.

3.2 Introduction

The world's population is rapidly graying, which holds significant implications for the mental-health profession. As they age, older adults have been shown to exhibit a gradual decline in working memory and performance on selective attention tasks [2] as well as gross anatomical changes, such as reductions in prefrontal cortical (PFC) volume [54, 4] and white-matter integrity that may be associated with cognitive function [1]. The functional consequences of these anatomical changes are not yet completely understood [54, 2] but have been shown to be related to changes in the attentional circuitry [3, 5, 6] of both humans [9] and primates [21, 55]. These attentional networks perform a wide variety of heterogeneous functions [56, 57], however, the focus of this study will be their role in goal-directed, or top-down, attention-based modulation of the visual associative cortex (VAC) and their role in healthy, normal aging [1, 15, 7, 3].

By monitoring the modulation of sensory cortical activity, changes in the sensory responses to external stimuli associated with goal-directed attention can be observed. Two divergent processes characterize this top-down, or goal-driven, modulation: in-

creased cortical responses to task-relevant stimuli (i.e. enhancement) and decreased cortical responses to task-irrelevant stimuli (i.e. suppression) [12, 10, 11, 36]. This modulation is not thought to originate from these local sensory cortical regions but rather arises from a distributed network of regions across the entire brain [22].

Early primate work has shown that the responses of individual sensory neurons can be modulated by attentional processes [10, 36] and that the prefrontal cortex (PFC) may play an important role in this modulation of activity [21, 55]. Additionally, primate PFC lesion studies showed that disruption of PFC function not only reduces cell-tuning specificity, but also produces a reduction in behavioral performance during a selective attention task [21]. This result has been observed in human populations either via stroke-induced PFC lesions [20] or, relevant to the study presented below, in healthy, older adults (60+ years old) [3]. In both of these populations, subjects show a significant reduction not only in task-performance but in neural markers of attentional modulation as well. Given the evidence of age-related PFC damage, it is likely that age-related changes to PFC function are a major source of age-related cognitive decline.

Older adults show an increase in PFC activation [58, 59, 60, 6], which is believed to be a compensatory mechanism for structural changes that occur during normal aging [61, 58]. These structural changes consist of: decreases in PFC cortical volume [2, 4] and reduction in frontal white-matter integrity [1], and provide a likely candidate mechanism for age-related reduction of neural suppression of task-irrelevant stimuli [3] and the associated age-related behavioral and cognitive deficits.

Since direct cortical-cortical connections between the PFC (source of modulation) and VAC (site of modulation) exist [16], these areas may form a functional network important for attention modulation. In recent years, there has been an accumulation of studies directed at exploring how large-scale brain networks are involved in goal-directed behavior and in non goal-directed activities (i.e. when participants are at rest). Two networks that have generated extensive interest are the frontal-

parietal network (or dorsal attention network) [35, 26, 27] and the default network [28, 27, 29]. The frontal-parietal network includes regions in the PFC, inferior frontal junction (IFJ), supplementary motor area (SMA), and superior intraparietal sulcus (sIPS) [27] and is co-activated during a wide-array of goal-directed tasks, including selective attention [35, 40], visual search [41], and WM [15]. The default network is made up of a distinct network of regions: the medial prefrontal cortex (mPFC); medial, lateral, and inferior parietal cortex (mPC, lPC, and iPC); retrosplenial cortex (ReSp); and the posterior cingulate cortex (PCC) [42] and was first described as a set of regions that were de-activated during goal-directed behavior [29]. However, the default network has been further implicated as an ensemble of regions functionally connected at rest that are activated during introspective cognitive functions, such as prospective and retrospective memory and internal monitoring [30, 31]. Thus, in a manner that parallels top-down enhancement and suppression in sensory cortices, distinct sets of parietal and frontal regions exhibit enhanced and suppressed activity dependent on the cognitive state of the individual. Given that previous results have shown both a differential role for both the frontal-parietal and default networks in attention allocation (Chapter 2) and a reduction in top-down modulation in healthy, older adults specific to suppression [3], the hypothesis is that age-related changes in the default/suppression network underlie age-related cognitive decline.

Neither the neural nor anatomical basis of the age-related selective suppression deficit has been established. However, previous studies have linked changes within the default mode to age-related cognitive deficits [1]. It has been demonstrated that older adults show both weakened task-induced deactivation [46] and increased disorganization [33, 34] of the default network compared to healthy, young controls and that these default network deficits are particularly pronounced under high cognitive load conditions [32]. The purpose of the study presented below was to determine if age-related default network changes (both functionally and anatom-

ically) are the basis of age-related cognitive deficits and the age-related selective suppression deficit. Using a working memory, selective attention fMRI task where participants were placed under a high cognitive load by having to simultaneously attend to and ignore task specific stimuli, the study below was able to extract neural markers of both enhancement and suppression while simultaneously assessing the integrity of the default/suppression network in both healthy, young controls and healthy, older participants. The results strongly support the hypothesis that anatomical and functional changes within the suppression network underlie the observed age-related cognitive deficits.

3.3 Results

3.3.1 Behavioral

To investigate the effects of aging on performance, both working memory accuracy (WM) and response time (RT) data from all conditions (Fig. 3.1: Remember Faces (FM); Remember Faces, Overlapped (FM-O); Remember Scenes, Overlapped (SM-O); and Remember Scenes (SM)) were subjected to a 2x2x2 ANOVA (with age, overlap vs. non-overlapped conditions, and stimulus type: faces vs. scenes as factors) separately for WM and RT. Analysis of WM data (Fig. 3.2A) revealed a main effect of aging ($F_{1,40} = 14.27$, $p < 0.0005$) such that younger participants showed significantly better WM performance compared to older participants. In addition, there also existed a main effect of overlap vs. non-overlapped conditions ($F_{1,40} = 117.11$, $p < 0.0001$) where all participants showed better WM performance on conditions where there were no overlapped stimuli (FM and SM) compared to those with overlapped stimuli (FM-O and SM-O). However, there existed no interaction at the group level between the two factors. That is to say, older participants did not show a significant change in the magnitude of the decrease in performance

between overlapped and non-overlapped conditions as compared to the healthy, young controls ($F_{1,40} = 1.51$, $p = 0.2$). There were also no significant differences between conditions where participant instructions were to attend to faces (FM and FM-O) or attend to scenes (SM and SM-O) ($F_{1,40} = 3.05$, $p = 0.09$). Thus, older adults performed worse across all conditions but when the older populations was tested as a homogeneous group the analysis did not reveal the age by overlap interaction that would be expected from a selective deficit in suppression. It is only by addressing changes in individual older adults that the selective deficit in suppression becomes clear during the WM task (below).

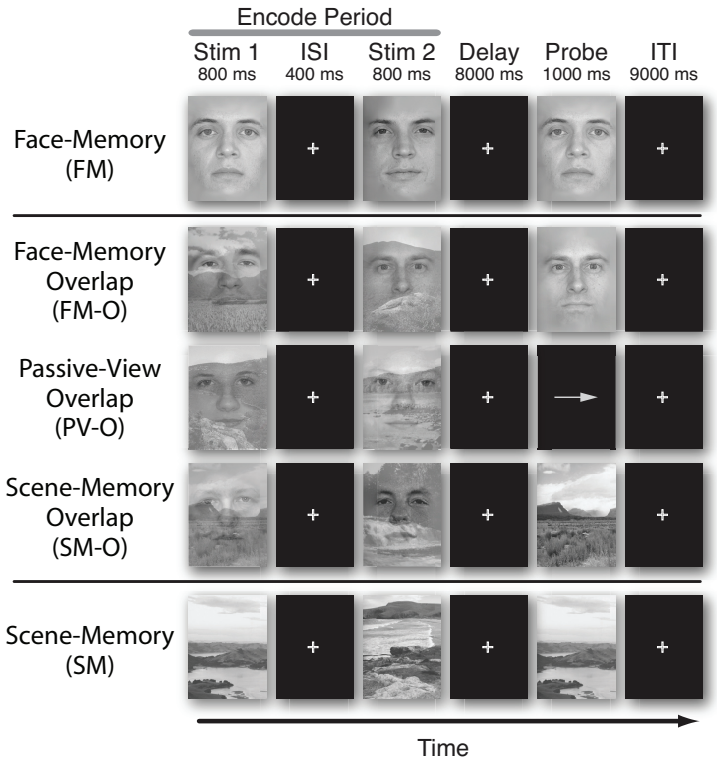

Figure 3.1: *Experimental Paradigm.* Participants were instructed to remember stim1 and stim2 and answer with a button press if the probe image matched either of the previous two stimuli. Participants were instructed to maintain fixation on the white crosshairs between stimuli and trials.

Similar results were observed for RT (Fig. 3.2B). Main-effects were observed for both aging ($F_{1,40} = 4.70$, $p < 0.04$) and overlap vs. non-overlapped conditions ($F_{1,40} = 62.53$, $p < 0.0001$) where older participants performed significantly worse

across all conditions as compared to young controls and all participants were affected by the presence of overlapped stimuli. However, as with the WM data above, there was no interaction between age and overlap vs. non-overlapped conditions ($F_{1,40} = 0.55$, $p = 0.5$).

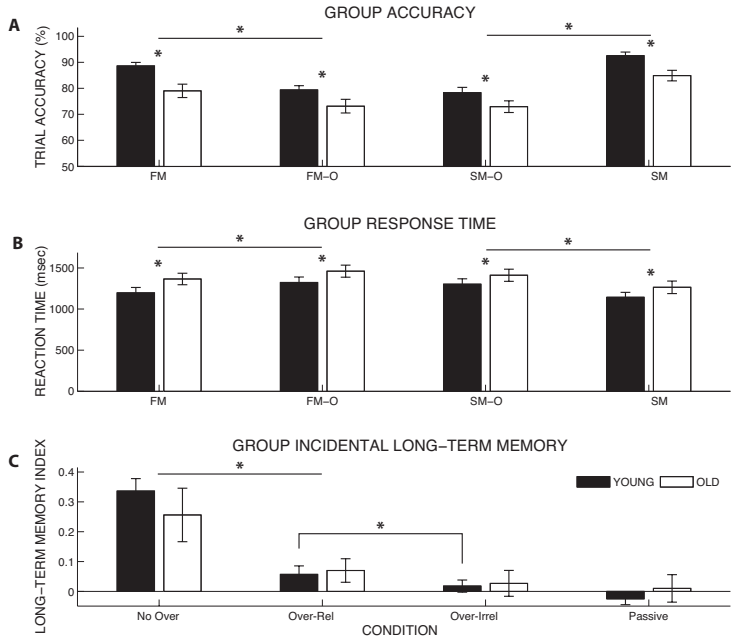

Figure 3.2: *Behavioral Results.* A) Working Memory (WM) accuracy results for younger (black bars) and older (white bars) participants. B) Response time (RT) results for younger and older participants. C) Incidental Long Term Memory (LTM) results for younger and older participants. All results were subjected to ANOVAs and post-hoc t-tests corrected for multiple comparisons. Error bars are standard error, $^*p < 0.05$.

Analysis of incidental long-term memory recognition performance (Fig. 3.2C) revealed that both young and older adults remembered Relevant-No-Distractor stimuli (stimuli from the FM and SM conditions collapsed across stimuli type – faces or scenes) significantly better than all other categories (young: $t_{20} = 5.86$, $p < 0.0001$; older: $t_{15} = 2.27$, $p < 0.04$; see methods section for category definitions). However, only younger participants displayed any statistical difference between the remaining three categories: Relevant-With-Distractor > Distractor > Passive-View (young: $t_{20} = 2.10$, $p < 0.05$ and $t_{20} = 2.09$, $p < 0.05$, and older: $t_{15} = 0.92$, $p = 0.4$ and $t_{15} = 0.26$, $p = 0.8$, respectively), indicating that task instructions – or top-

down effects – affected younger participants incidental long-term memory scores for task-relevant vs. task-distracting stimuli but not for older participants. Thus, while older adults did not have a selective deficit in the distractor task (instead showing generally decreased performance on all tasks) they remembered distractor information at the same rate as task-relevant information, indicating a deficit in the suppression of task-irrelevant information.

3.3.2 Univariate ROI Results

To compare the top-down effects of task-goals (instructions) on visual processing, neural measures were derived by modeling encoding-period activity using a GLM and extracting β values associated with activations from a scene-selective regions of interest (ROI), parahippocampal place area, (PPA) and a face-selective ROI, fusiform face area (FFA). Specifically, the left PPA and right FFA were used, as previous studies show these are the most robust regions of face and scene selective activity modulation [12]. We found that both in the FFA and PPA, which are selective to face and scene processing, respectively, encoding period activation of these regions follows the attentional demands of the task. Younger participant data from the PPA revealed the expected bottom-up scene-selectivity of this region, such that stimuli that include scenes alone demonstrated significantly greater responses than stimuli with faces alone (SM > FM: $t_{21} = 9.45$, $p < 0.0001$) (Fig. 3.3A). In addition, there was a significant top-down modulation effect, such that all three overlapped conditions revealed significantly different patterns of activation depending on the goals of the task: enhancement of PPA activity when scenes were relevant compared to passive-view baseline (SM-O > PV-O; $t_{21} = 3.33$, $p < 0.003$), and significant suppression of PPA activity when scenes were irrelevant compared to baseline (FM-O < PV-O; $t_{21} = 2.34$, $p < 0.03$). These three levels of activation (SM-O > PV-O > FM-O) represent a pure, top-down effect because bottom-up information was constant across tasks. In addition, the magnitude of the ROI effects

for the overlapped conditions fell between the levels attained in pure conditions (SM > SM-O > PV-O > FM-O > FM). A similar pattern of activation was observed for the FFA (Fig. 3.3B). A significant bottom-up effect was demonstrated, such that FM > SM ($t_{21} = 5.55$, $p < 0.0001$), as well as significant enhancement (FM-O > PV-O: $t_{21} = 4.08$, $p < 0.0001$). However, there was not a significant measure of suppression within the FFA (SM-O < PV-O: $t_{21} = -1.84$, $p = 0.08$), consistent with a previous finding investigating enhancement and suppression within the VAC [12].

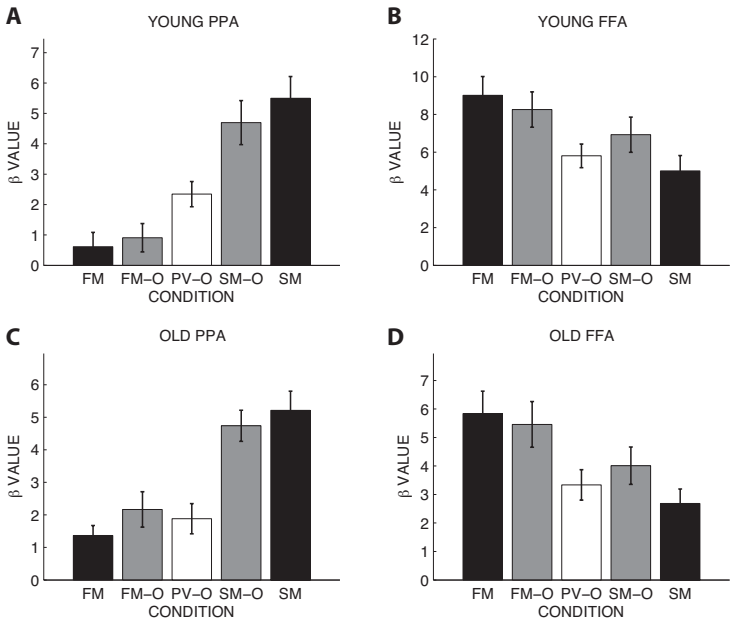

Figure 3.3: *Univariate VAC ROI Results.* The encode period activity for A) younger PPA, B) younger FFA, C) older PPA, and older FFA VAC ROIs. All results were subjected to ANOVAs and post-hoc t-tests with multiple comparisons. Error bars are standard error, $^*p < 0.05$.

The data from the older participants showed significant enhancement of task-relevant stimuli (mirroring the younger data above) but did not show significant suppression of task-irrelevant stimuli both within the PPA and FFA (Fig 3.3C and 3.3D, respectively) [3]. PPA data showed selectivity for pure scenes (SM) compared to pure faces (FM) such that scenes elicited a greater response than faces (SM > FM: $t_{18} = 7.57$, $p < 0.0001$). In addition, older participants demonstrated neural enhancement to scenes when overlapped scenes were task-relevant compared

to passive (SM-O > PV-O: $t_{18} = 7.83$, $p < 0.0001$). However, there was no observed top-down suppression of PPA when scenes were task-irrelevant compared to passive (FM-O < PV-O: $t_{18} = -0.47$, $p = 0.6$) consistent with previous studies demonstrating an age-related suppression deficit wherein older participants do not robustly demonstrate neural suppression of task-irrelevant visual stimuli [3]. Since the above experimental paradigm has a direct measure of PPA selectivity (SM vs. FM, a pure stimulus-driven, or bottom-up effect), the top-down (or goal-driven) effects (SM-O vs. PV-O vs. FM-O) may be normalized to each participant's stimulus selectivity. Even when the measure of suppression (PV-O – FM-O) is normalized by selectivity (SM – FM), there is still no significant measure of suppression for older participants ($t_{18} = -0.77$, $p = 0.3$). Similar results were shown for the FFA as compared to the healthy, young controls. Older adults showed a face-selectivity for the FFA (FM > SM: $t_{18} = 6.38$, $p < 0.0001$) as well as enhancement when overlapped faces were relevant compared to passive (FM-O > PV-O: $t_{18} = 4.20$, $p < 0.0005$) but did not demonstrate suppression of the FFA when faces were irrelevant compared to passive (SM-O < PV-O: $t_{18} = -1.52$, $p = 0.1$). Since the PPA exhibited the most robust marker of both enhancement and suppression for healthy, young controls, only data from the PPA will be analyzed further.

Data from the PPA ROI were directly compared between healthy, younger and older participants using t-tests. Younger and older participants did not show significantly different measures of enhancement at the group level (Fig. 3.4A, SM-O > PV-O: $t_{39} = -0.60$, $p = 0.6$) even when normalized to bottom-up selectivity (SM – FM) (Fig. 3.4B, $t_{39} = -0.45$, $p = 0.7$) but did show different degrees of suppression where young participants showed weakly (yet, significantly) greater suppression than older participants (Fig. 3.4C, one-tailed, $t_{39} = 1.98$, $p < 0.03$) duplicating the previously described *age-related selective suppression deficit* [3]. Importantly, this age-related selective suppression deficit holds even if normalized to bottom-up selectivity (Fig. 3.4D, one-tailed, $t_{39} = 1.89$, $p < 0.03$), demonstrating that the

observed effect is not driven by a loss of VAC selectivity.

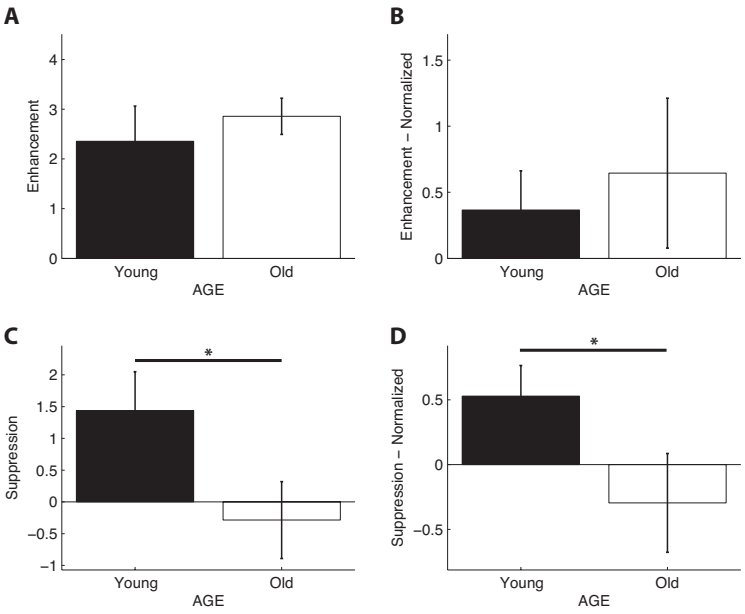

Figure 3.4: *PPA Enhancement and Suppression Indices.* Normalized. A) Comparison of younger (black bars) and older (white bars) enhancement index (SM-O – PV-O). B) Same as A but normalized to bottom-up differences (SM – FM). C) Comparison of younger and older suppression index (PV-O – FM-O). D) Same as C but normalized to bottom-up differences (similar to B). Error bars are standard error, $^*p < 0.05$.

3.3.3 Relationship Between Behavioral Performance and Suppression

Given that older participants showed an age-related suppression deficit, the fact that they did not show an age-related differential WM impact of distraction (i.e. overlapped vs. non-overlapped conditions) was unexpected. However, older adults generally show increased behavioral heterogeneity compared to healthy, young controls [2]. It is plausible to speculate that even though both the suppression deficit and lack of an age-related behavioral impact of distraction were shown at the group level, some older participants were differentially impacted by distraction and that these participants also showed a greater suppression deficit as compared to their peers. To explicitly test this hypothesis, an across subject correlation was per-

formed separately on younger and older participants between participants' magnitude of suppression and WM performance. Older adults showed a positive correlation between WM performance on the remember faces, overlap condition (FM-O) and their measure of PPA suppression (PV-O – FM-O) (Fig. 3.5A: $r = 0.47$, $p < 0.04$) such that older participants that showed the greatest suppression also showed the best WM performance on the FM-O condition. Notably, this relationship does not exist for younger participants (Fig. 3.5B: $r = 0.13$, $p = 0.6$). Perhaps more telling, when performance on the remember faces, overlapped condition was normalized to performance on the remember faces, non-overlapped condition (FM-O – FM), the relationship between magnitude of suppression and maintenance of performance when presented with distraction was maintained for older participants (Fig. 3.5C: $r = -0.63$, $p < 0.004$) but not younger participants (Fig. 3.5D: $r = -0.22$, $p = 0.3$). This result strongly supports the hypothesis that successful suppression is key to maintenance of performance when task-irrelevant information is present [14] and is consistent with previous results showing that the degree of suppression is predictive of WM performance in healthy, older adults [3]. Oddly enough, younger participants did not show this relationship. It is possible that younger participants are performing at or near ceiling and are not sufficiently challenged to maximize gain from successful suppression whereas top-down modulation has previously been shown to saturate more quickly with task difficulty in older participants [32]. Additionally, it is possible that both the neural and behavioral measures were too homogenous within the healthy, young controls to extract a meaningful correlation. Since older adults show not only changes in neural activations as compared to healthy, young controls but also neuro-anatomical changes as well (particularly gray-matter atrophy), it is useful to investigate if both the behavioral and neural heterogeneities observed above have a basis in underlying changes in anatomy.

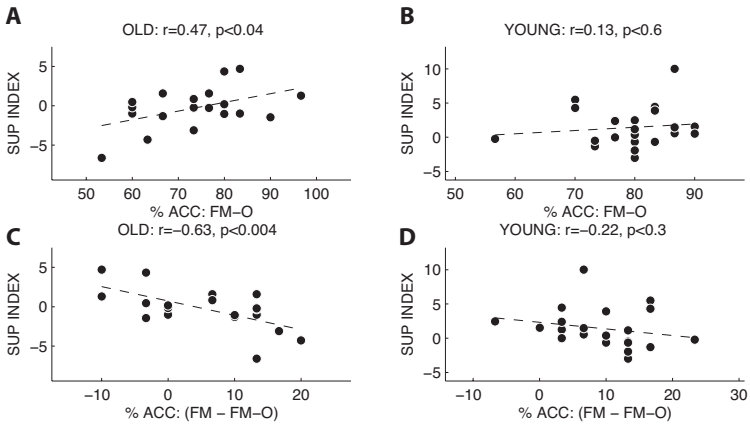

Figure 3.5: *Neural-Behavioral Correlations.* A) Correlation between WM accuracy in remember faces, overlap (FM-O) condition and older participants' suppression indices (PPA: PV-O – FM-O). B) Same as A but using younger participants' data. C) Correlation between the difference in WM accuracy with and without overlapping images (FM – FM-O) and older participants' suppression indices. Same as C but using younger participants' data.

3.3.4 Relationship between Gray-Matter Atrophy and WM Performance

To probe for regions of gray-matter atrophy that are associated with decreased performance in older participants when challenged with task-irrelevant information, a voxel-based-morphometry (VBM) analysis was performed. A whole-brain, across subject correlation was performed between gray-matter volume, as a rough correlate of gray-matter atrophy [62, 63], and the WM impact of task-irrelevant information (using FM – FM-O so as to correspond to the VBM analysis using PPA suppression below). The results yielded regions where gray-matter atrophy is associated with decreased WM performance when presented with task-irrelevant information (Fig. 3.6A). Atrophy within the medial prefrontal cortex (mPFC) was shown to be significantly associated with the impact of task-irrelevant information on WM performance. These results indicate that older participants who have increased atrophy within the mPFC (compared to their peers) are the same participants who show the greatest WM impact of task-irrelevant information the significance of which is discussed in the context of the "Suppression Network" sec-

tion below (section 3.3.6).

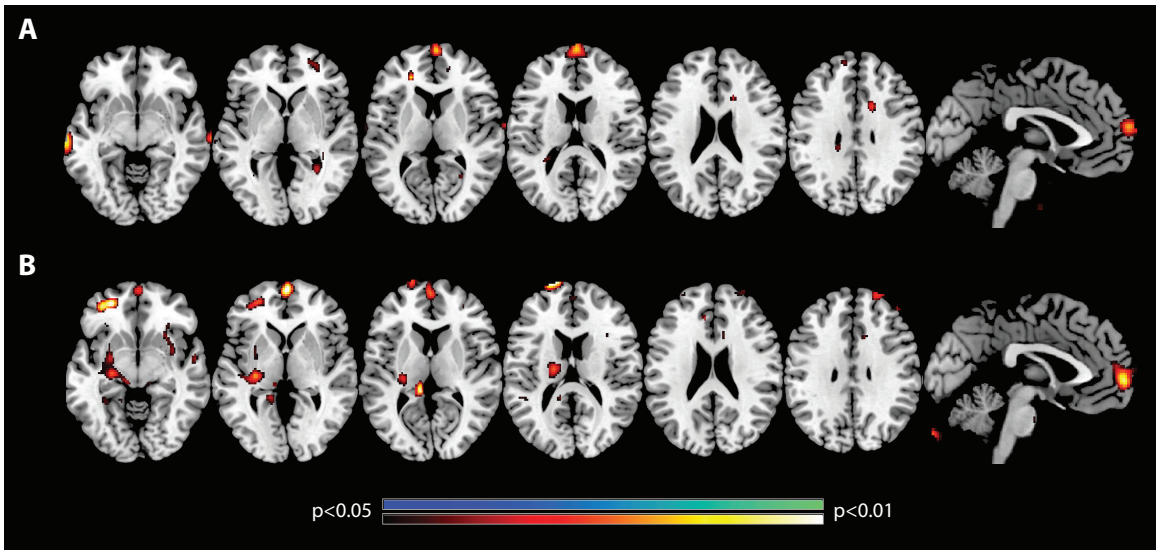

Figure 3.6: *Voxel Based Morphometry Results.* A) Whole-brain correlation between the ratio of WM accuracy with and without overlapping images (FM-O / FM) and gray-matter volume in older participants. B) Whole-brain correlation between older participants' suppression indices (PPA: PV-O – FM-O) and gray matter atrophy. All images thresholded at $p < 0.05$ and corrected for multiple comparisons using cluster method described in Materials and Methods.

3.3.5 Relationship between Gray-Matter Atrophy and Neural Suppression

A VBM analysis was performed as above except that each older participant's magnitude of PPA suppression (PV-O – FM-O) was used as a test-variable against voxel-by-voxel gray-matter volume (Fig. 3.6B). As with the results above, a significant relationship was observed between the mPFC and the magnitude of each participant's PPA suppression: increased atrophy within the mPFC is associated with decreased suppression of the PPA when scenes were irrelevant (PV-O – FM-O). Taken together, both VBM results strongly implicate a relationship between integrity of the mPFC and both the maintenance of WM performance when presented with task-irrelevant information and the neural suppression of VAC regions that process task-irrelevant information. This finding is consistent with previous

studies from the lab demonstrating that the mPFC also plays a role in suppression of task-irrelevant information in healthy, young controls as defined by its position as node within the suppression network (Chapter 2).

3.3.6 Age-Related Changes to the Suppression Network

To investigate age-related changes to regions involved in suppression (the suppression network) (Chapter 2) functional connectivity maps were generated and compared across age groups. Capitalizing on trial-by-trial variability, whole-brain functional connectivity maps were assessed by correlating activity from the VAC ROIs (seed regions) with voxels from the rest of the brain [44]. Regions that are highly correlated with a VAC seed across trials are presumed to be functionally connected, thereby defining large-scale networks associated with activity modulation that occurs in those regions. By differentially pairing a seed with a task condition, enhancement and suppression networks can be evaluated. A suppression network map was generated by contrasting the PPA connectivity maps obtained in the FM-O and PV-O contrast (i.e., comparing the condition when scenes were behaviorally irrelevant, to the condition when there were no attentional demands). One advantage of contrasting the FM-O and PV-O functional connectivity maps is that bottom-up (or stimulus driven) information is held constant across conditions and only top-down (or goal driven) effects remain. Brain regions more strongly correlated with the PPA in FM-O compared to PV-O are potentially associated with suppression processes. It is important to note that these analyses are correlational and do not reveal that the suppression network regions are sources of top-down control, but rather that they are associated with VAC regions that are suppressed.

In younger participants, regions such as the mPFC, posterior cingulate cortex (PCC), retrosplenial cortex (ReSp), and bilateral parietal cortex (PC) were func-

tionally coupled with the PPA during suppression and comprise the previously described suppression network (Chapter 2) (Fig. 3.7A). However, when the same analysis is performed on the older participants, the mPFC is not associated with the suppression network (Fig. 3.7B). This difference in mPFC coupling between younger and older participants is significant (Fig. 3.7C). Taken with the results above, this clearly demonstrates that not only is suppression significantly reduced in older participants compared to healthy, young controls, but that the putative suppression network is also significantly altered in older participants.

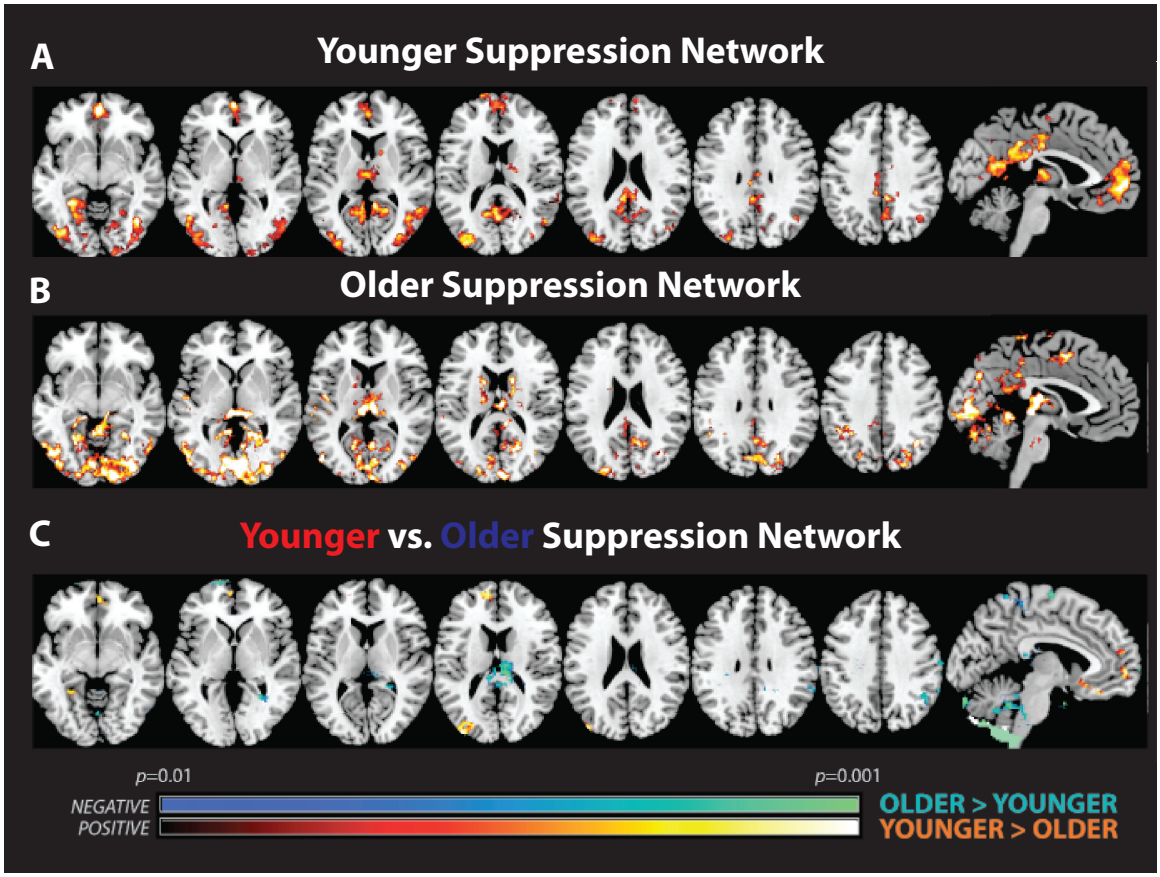

Figure 3.7: *Younger vs. Older Suppression Network.* A) Functional connectivity map for younger participants for the PPA, contrasting (FM-O > PV-O, i.e. suppression). B) Same as A but using older participants' data. C) Contrast between younger and older suppression maps. All images thresholded at $p < 0.05$ and corrected for multiple comparisons using cluster method described in Materials and Methods.

Previous results demonstrated that the magnitude of coupling between the mPFC and the PPA during suppression was predictive of the magnitude of suppression

in healthy, young controls (Chapter 2). However, this relationship does not exist with older participants, increased PPA-mPFC coupling is not predictive of a participant's degree of PPA suppression consistent with the finding of an age-related selective suppression deficit.

3.3.7 Age-Related Alterations to the Default Network

In addition to being involved in the suppression network as described above, the mPFC also plays an important role within the default network [28, 27, 29]. Previous results from the lab implicated a role of the default network in successful suppression of task-irrelevant information in that the suppression network and the default network may be one and the same (Chapter 2).

To determine whether the age-related changes to the suppression network are consistent with both its additional role as the default network and age-related changes to the default network [33, 46, 34], the default network was derived using an independent localizer task (see Materials and Methods) for both the healthy, young controls and the older participants (Fig. 3.8). Analysis of the young participants showed the canonical default network [28, 27, 29] consisting of mPFC, PCC, and bilateral PC (Fig. 3.8A) while older participants did not show task-induced deactivation of the mPFC (Fig. 3.8B) supporting the result that the mPFC is not associated as strongly with the default network in older participants [42, 31] as compared to healthy, young controls (Fig. 3.8C). Taken together with the above results showing mPFC atrophy is related to decreased WM performance and decreased neural suppression, and that mPFC is not associated with the suppression network in older participants, mPFC dysfunction may play a role in the cognitive effects of healthy, normal aging.

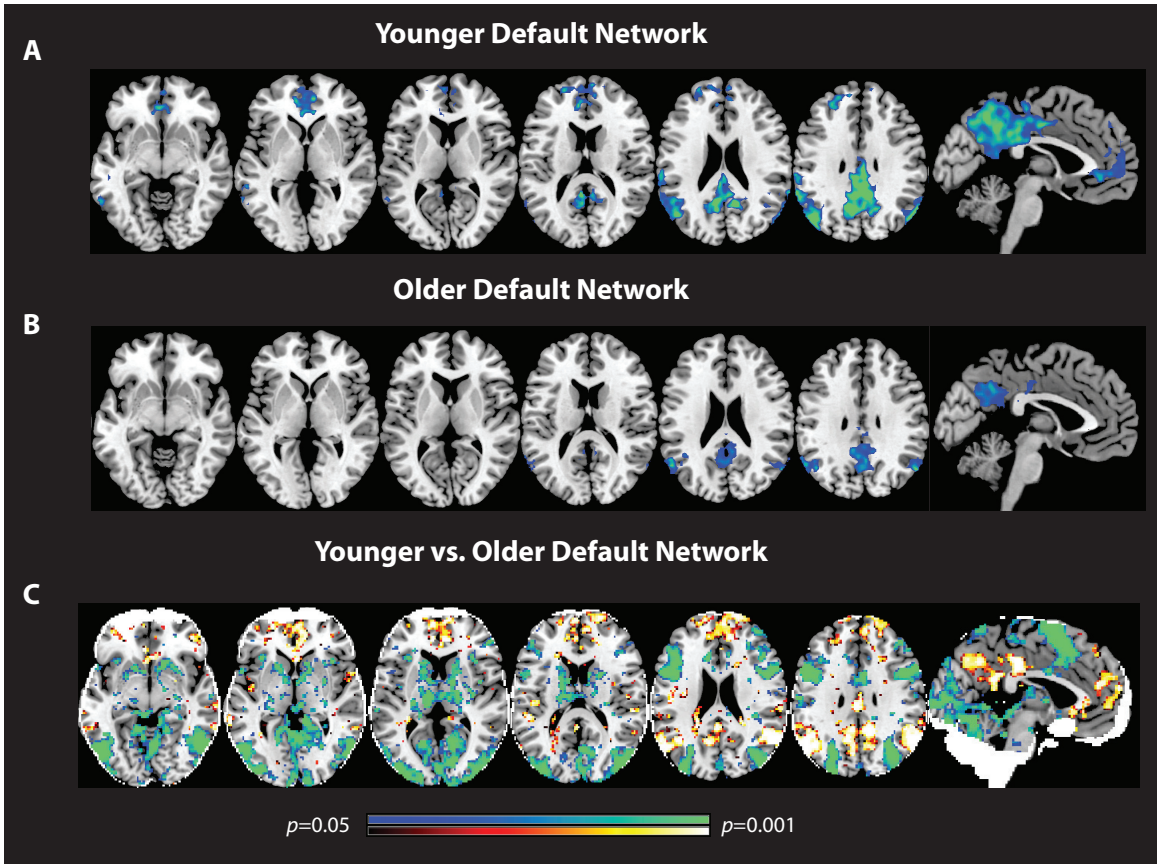

Figure 3.8: *Younger vs. Older Default Network.* A) Whole-brain analysis showing regions with significantly greater activity at rest during independent localizer task (REST > TASK) for younger participants. B) Same as A but using older participants' data. C) Contrast between younger and older participants' default network maps. All images thresholded at $p < 0.05$ and corrected for multiple comparisons using cluster method described in Materials and Methods.

3.3.8 Default Network Deactivation and Age-Related Neural and Behavioral Changes

To test the hypothesis that age-related dysfunction of the default network is related to the neural and behavioral effects described above, an across subject-subject correlation was performed using task-induced mPFC suppression (PV-O – FM-O) as a metric of default network functionality. When default network deactivation is correlated with WM responses in the face of distraction (FM – FM-O), there is a clear relationship in older adults where those adults that show more task-induced mPFC suppression, show the greatest maintenance of WM performance

(Fig. 3.9A: $r = -0.47$, $p < 0.04$). This relationship is not observed in healthy, young controls (Fig. 3.9B: $r = -0.23$, $p = 0.3$). In addition, when the comparison is made between mPFC suppression and PPA suppression, older adults again show a clear relationship where those that show maximum mPFC suppression also show maximum PPA suppression (Fig. 3.9C: $r = 0.51$, $p < 0.02$) which is not observed in healthy, young controls (Fig. 3.9D, $r = 0.14$, $p = 0.5$). Taken together, these results demonstrate a clear relationship between mPFC/default network dysfunction and the neural and behavioral manifestations of cognitive aging.

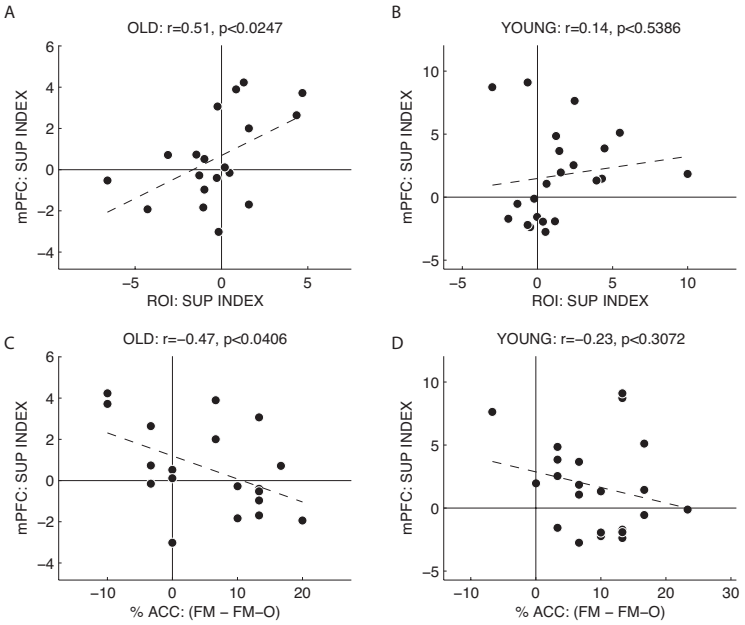

Figure 3.9: *Relationship Between Default Network Suppression and Performance.* Correlation between default network suppression (PV-O – FM-O) and WM distraction (FM – FM-O) in older (A) and younger (B) participants. Correlation between default network suppression and PPA suppression (PV-O – FM-O) in older (C) and younger (D) participants.

3.4 Discussion

This study provides the first evidence directly supporting the hypothesis that age-related changes to the default network directly affect sensory processing in healthy, older adults. Specifically, the results presented above show that older adults who

are better able to suppress task-irrelevant sensory information are those that are least impacted by distraction; a relationship that does not exist for healthy, young controls. In addition, both behavioral and neural measures of distractibility (i.e. comparison of WM performance on overlapped vs. non-overlapped conditions and suppression) were correlated with gray-matter atrophy within the mPFC, a key node of the default network, such that older adults with greater mPFC atrophy showed decreased WM performance and decreased levels of suppression. Since the mPFC has been shown to be involved both as a node of the default network and a node of the suppression network (Chapter 2), these results present a novel association between age-related structural changes and age-related neural and behavioral decline.

3.4.1 Behavioral Analysis

At the group level, older adults did not show a greater impact of the addition of task-irrelevant information compared to healthy, young controls (Fig. 3.2) despite showing an age-related decline in performance across all tasks consistent with a similar study [3]. This result was especially puzzling given the age-related selective suppression deficit described both here (Fig. 3.3) and elsewhere [3] where older adults did not show significant reductions in neural activity associated with task-irrelevant information compared to healthy, young controls consistent with the finding that older adults showed similar LTM scores for both task-relevant and task-irrelevant stimuli. However, this result may be explained by the profound heterogeneity found in older participants' responses compared to controls. It is likely that some of the older participants did show an age/overlapped-stimuli interaction but that the effect of these low performers were washed out at the group level. To investigate this, a correlation was performed between the magnitude of suppression and the magnitude of the performance decrement associated with the addition of task-irrelevant information. Consistent with previous findings [3], older adults who

showed the least suppression of task-irrelevant information were those who showed the greatest reduction is performance on the conditions with overlapped stimuli compared to those without (Fig. 3.5). This finding did not hold for healthy, young controls which may reflect the hypothesis that younger adults maintain greater neural processing resources and are more efficiently able to maintain neural processes compared to healthy, older adults [9].

3.4.2 Age-Related Selective Suppression Deficit

One theory of cognitive aging holds that older adults develop an implicit reduction in their ability to divert attention away from task-unrelated, distracting elements [64, 65]. Previous results from a similar experiment [3] are consistent with the inhibitory deficit hypothesis. In this study, the authors demonstrated that older participants had elevated levels of neural activity associated with task-irrelevant stimuli compared with younger participants while, at the same time, older participants were able to maintain the process of enhancement providing further evidence that both enhancement and suppression are neurally distinct processes. Furthermore, the authors showed that the magnitude of this suppression deficit was predictive of behavioral performance; older participants who performed best on the task had greater degrees of suppression of the irrelevant VAC regions compared to their peers just as found above. However, one difficulty in interpreting this age-related selective suppression deficit is that VAC becomes less selective (decreased bottom-up modulation) with age [66]. Thus one possible explanation for the observed loss of suppression in older adults is that it could be related to bottom-up (or stimulus-driven) sensory processing rather than top-down (or goal-driven) modulation. However, the above paradigm is able to distinguish between these possibilities using the two non-overlapping stimulus conditions (Fig. 3.1, FM and SM). Since both these conditions represent a pure stimulus-driven effect, the top-down effects (FM-O vs. PV-O vs. SM-O) can be normalized against the bottom-up changes

(FM vs. SM) to determine if the age-related selective suppression deficit is solely due to loss of selectivity within the VAC. The results support the hypothesis that the age-related suppression deficit is not due to an age-related loss of selectivity but rather due to changes in top-down processing that may be associated with age-related deficits in distal brain regions.

3.4.3 mPFC Atrophy, WM and Suppression Impairment

A wide variety of brain regions show increased atrophy with age, particularly within the PFC [2]. Using VBM, the results above demonstrate that WM impairment in the face of distracting, task-irrelevant information is associated with increased atrophy within the mPFC. As hypothesized, this increased mPFC atrophy is also associated with decreased neural suppression of task-irrelevant information where older participants with high levels of mPFC atrophy both perform worse when distracting information is present and show decreased ability to neurally suppress task-irrelevant information. Granted that both fMRI and anatomical approaches are purely correlative and do not demonstrate causality; however, it seems likely that anatomical changes within the PFC (particularly the mPFC) may be driving age-related performance and neural declines. Previous studies have also implicated a role of mPFC dysfunction is age-related behavioral decline, specifically, that failure to induce task-related deactivations of mPFC is associated with the effects of cognitive aging (such as reduced WM capacity) in healthy, older populations [67]. Notably, the mPFC has also been shown to functionally associated with the suppression network in healthy, young controls (Chapter 2). Thus, it is unsurprising that mPFC dysfunction is associated with suppression deficits in healthy, older participants.

3.4.4 Age-Related Changes to the Suppression Network

Previous findings demonstrated that there exist separate functional networks differentially associated with enhancement and suppression in healthy, young controls (Chapter 2). The neural process of enhancement was correlated with the previously described frontal-parietal network while suppression was correlated with the default network. Since the univariate ROI results in Fig. 3.3 show a deficit only for suppression in older participants, it was useful to directly compare the suppression network for both younger and older participants. Results directly comparing the derived suppression network for both the young controls and the older participants (Fig. 3.7) showed that older adults have greater dysfunction within the suppression network. In particular, older participants did not have as extensive suppression network as did healthy, young controls and the mPFC was not correlated at all with activity with VAC regions processing task-irrelevant information consistent with the age-related selective suppression deficit observed: not only was there a reduction in VAC suppression, but the suppression network itself was deficient in healthy, older participants. Taken together with 1) previous findings showing mPFC is related to processing of task-irrelevant information and suppression in healthy, young controls and 2) mPFC atrophy is associated with neural and behavioral impairments in older adults, the above results present a model where mPFC atrophy in older adults is at the root cause of changes to the suppression network resulting in the age-related selective suppression deficit and the corresponding performance decrement associated with aging. However, since the mPFC is associated not only with the derived suppression network, but with the default network as well, mPFC dysfunction in older adults may also be measured via changes in the default network.

3.4.5 Age-Related Changes to the Default Network

There have been numerous studies of default network integrity with healthy, normal aging. In healthy, young controls, the default network is selectively deactivated by external, attentionally demanding tasks [28], while at the same time it is activated by internally generated tasks such as prospective memory and "mind-wandering" [28, 31]. Older adults show decreased deactivations is response to externally demanding tasks [46] while also showing much smaller and fewer regions that are co-activated as nodes in the default network [33, 34]. In addition, both the functional and anatomical fidelity of the default network is associated with general symptoms (decreases in working memory and executive function) of age-related cognitive decline where older adults with decreased default network organization exhibit larger cognitive deficits than their peers [1]. Using the dataset above, the default network was derived for both younger and older participants (Fig. 3.8) and it was found that older participants show a significantly reduced default network activation pattern, particularly within the mPFC, consistent with both the mPFC atrophy and loss of mPFC functional connectivity within the suppression network in healthy, older participants.

3.5 Conclusion

The results presented above demonstrate that successful suppression of task-irrelevant information is associated with successful performance in healthy, older adults, supporting previous findings demonstrating the existence of the age-related selective suppression deficit [3]. Furthermore, this study also provides the first evidence demonstrating that the link between mPFC atrophy and the age-related selective suppression deficit. Interestingly, the mPFC has already been shown to be associated with both the suppression network and default network in healthy, young controls, and it is not surprising that an age-related disruption of a suppression

network node results not only in decreases in neural suppression but also disruptions of behavior in the face of distracting, task-irrelevant information. The overlap between the suppression network and the default network elucidates findings that normal aging is associated with both a deficit in suppressing external irrelevant information [3] and a decreased ability to deactivate the default network during tasks [46]. This may represent further evidence of a relationship between these networks and a possible mechanistic basis to account for age-related suppression deficits.

3.6 Materials and Methods

3.6.1 Participants

Functional and high-resolution anatomical MRI images were obtained from 22 healthy young participants (ages: 18-34, mean: 23.7, females: 11) and 20 healthy, older participants (ages: 61-81, mean: 70.8, females: 11) while performing the task described below. Participants were recruited and compensated monetarily as per the UCSF Committee on Human Research (CHR) approval. All participants had normal or corrected-to-normal vision and were taking no psychotropic medications. One younger and one older participant were excluded from all analysis due to excessive motion artifacts ($>$ 3 mm) within the scanner.

3.6.2 Neuropsychological Testing

Prior to the experiment, older adults were administered a battery of thirteen neuropsychological tests. Participants were required to score within two standard deviations of age-matched control values on these tests to be included in the study. The neuropsychological evaluation consisted of tests designed to assess general intellec-

tual function [68], verbal learning (CVLT-II), geriatric depression (GDS), visual-spatial function (modified Rey-Osterrieth figure), visual-episodic memory (memory for details of a modified Rey-Osterrieth Complex Figure (ROCF) [69, 70], visual-motor sequencing (trail making tests A and B), phonemic fluency (words beginning with the letter D'), semantic fluency (animals), calculation ability (arithmetic), executive functioning [71, 72], working memory and incidental recall [73, 74] backward digit span and digit symbol, and WAIS-R [71].

3.6.3 Experimental Design

The experimental paradigm comprised five similar tasks in a delayed-recognition WM task design (Fig. 3.1), similar to previously published work [13]. Each task consisted of the same basic temporal sequence with only the instructions differing across tasks. All tasks involved viewing two images (Stim1, Stim2), each displayed for 800 ms (with a 400 ms inter-stimulus interval [ISI]) followed by a 8 second period (Delay) in which the images were to be remembered and mentally rehearsed. After the delay, a third image appeared (Probe) for 1000 sec. The participant was instructed to respond with a button press (as quickly as possible without sacrificing accuracy) whether or not the Probe image matched either of the previous two images (Stim1 or Stim2). This was followed by an inter-trial interval (ITI) lasting 9 seconds.

For three of the five tasks, the Stim1 and Stim2 images were composed of both a scene and a face superimposed upon each other. Participants were instructed to focus their attention on and remember either the face or the scene, while ignoring the other. In the face memory-overlap task (FM-O), the faces were remembered while the scenes were ignored, and vice versa in the scene memory-overlap task (SM-O). When the Probe image appeared, it was composed of an isolated face in the FM-O task, and an isolated scene in the SM-O task. For the passive view

(PV-O) task, participants were instructed to view the overlapped images without trying to remember them, after which they responded to an arrow direction with a button press. For the other two tasks, the Stim1 and Stim2 images were composed of a single stimulus without any distracting/overlapping information: a face in the face memory task (FM) and a scene in the scene memory task (SM). The task was presented in 2 separate blocks, each block consisting of all 5 task sets counterbalanced in random order across all participants. Each task set consisted of 30 trials (60 total trials per task, 120 total Encode Period images).

Following the main experiment, participants performed a surprise post-experiment recognition test in which they viewed 320 non-overlapped images, including 160 faces and 160 scenes. 80 of the faces and 80 of the scenes were novel stimuli that were not included in the main experiment. There were 20 faces each from the FM, FM-O, SM-O, and PV-O tasks, and 20 scenes each from the SM, SM-O, FM-O, and PV-O tasks. No stimuli in the post-experiment test were seen more than once before. All included face and scene stimuli (both novel images and images from the experiment) were randomly ordered, and participants were asked to rate their recognition of each image on a scale from 1 – 4. For analysis of this data, each participant's ratings were collapsed across stimulus type and normalized to their average rating for novel stimuli. Scores were then collapsed across conditions and broken into the following categories: No-Overlap (stimuli from the SM and FM conditions), Overlap-Relevant (scenes and faces from the SM-O and FM-O conditions, respectively), Overlap-Irrelevant (faces and scenes from the SM-O and FM-O conditions, respectively), and Passive-View (faces and scenes from the PV-O condition). Post-experiment recognition test was not collected on 3 older participants due to time constraints.

3.6.4 Stimuli

All stimuli consisted of 225x300 pixel grayscale images, presented foveally, subtending a visual angle of 3° from a small cross at the center of the image. The face stimuli consisted of a variety of neutral-expression male and female faces across a large age range. Hair and ears were removed digitally, and a blur was applied along the contours of the face as to remove any potential non-face-specific cues. The gender of the face stimuli was held constant within each trial. Images of scenes were not digitally modified beyond resizing and grayscaling. For the tasks consisting of overlapped faces and scenes, one face and one scene were randomly paired, made transparent, and digitally overlapped using Adobe Photoshop CS2 such that both were equally visible. Overlapped and isolated images were randomly assigned to the different tasks.

3.6.5 Localizer and Default Network

To identify VAC regions maximally responsive to scenes and faces (the parahippocampal place area – or PPA – and the face fusiform area – or FFA, a localizer task independent of the main experimental task was performed, which consisted of 14 interleaved, 12 sec blocks of 20 scenes or faces with a 8 sec delay between each block [12]. To ensure participant's maintained vigilance, they were asked to press a button whenever they saw the exact same stimulus presented twice in a row (10% of stimuli presented). fMRI data was acquired and processed as described below. A contrast was created from the general linear model (GLM) β-maps for scenes and faces and the most active 35 voxels ($\backsim$0.390 cm^3) were selected from the approximate anatomical location for each of the following: left PPA (lPPA), right PPA (rPPA), left FFA (lFFA), and right FFA (rFFA) 12. Default network activity was functionally defined as regions where there was greater degree of activity during rest compared to 1-back [28]. ROIs for the default network were defined using

clusters of activity anatomically constrained to published coordinates of network nodes [28, 27].

3.6.6 fMRI Collection and Processing

All fMRI data were collected on a Siemens 3T MAGNETOM Treo 3T scanner with stimuli presented on an LCD monitor viewed in the prone position by participants using a mirror rigidly attached to the 12-channel head-coil. Echoplanar imaging (EPI) data was acquired ($FA = 90°$, $T_E = 25$ ms, $T_R = 2$ sec) with 33 interleaved axial slices (with a 0.5 mm gap) for a final resolution of 1.79x1.79x3.5mm/voxel ($FOV = 23$ cm; 128x128 matrix). All data preprocessing was conducted in SPM5 (Wellcome Department of Imaging Neuroscience, London, England). Raw blood oxygen level dependent (BOLD) data was corrected offline for slice-timing acquisition and motion-artifacts. A 5mm isotropic Gaussian smoothing kernel was applied using SPM5 prior to modeling the data. In addition to the EPI data, high-resolution T1-MPRAGE images (1x1x1 mm voxel size; FOV = 160 x 240 x 256 mm, $T_R = 2300$ ms, $T_E = 3$ ms, $FA = 90°$) were acquired to aid in anatomical localizations of activity and to screen for any undiagnosed neurological trauma.

Region of interest (ROI) activities were calculated by modeling the encoding (including both stimuli and the ISI), delay periods, and probe periods in each condition using a boxcar function convolved with the canonical hemodynamic response function (HRF) for the duration of each epoch as a general linear model (GLM) within SPM5. Native-space masks for each posterior ROI were created for each participant as described above and the estimated coefficients for encode-period activity were used as a measure of posterior VAC activations. Group-level univariate analysis was performed by normalizing each participant's mean EPI image to the Montreal Neurological Institute (MNI; 2x2x2 mm voxel size) template image prior to Gaussian smoothing and modeling.

3.6.7 VBM Analysis

Gray-matter atrophy was modeled by normalizing participants' T1-MPRAGE images into MNI-normalized space; segmented into gray-matter, white-matter, and cerebral spinal fluid maps, and smoothed using a 12mm isotropic Gaussian kernel in SPM5 as previously described [62, 63]. All images were manually inspected after segmentation. Correlations were performed on modulated gray-matter images with sex, age, and total-intracranial volume as nuisance variables. Resulting images were thresholded at $p < 0.05$ and corrected for multiple comparisons using the method described below.

3.6.8 Network Analysis

Functional connectivity network maps were created for each participant as described previously using a β-series correlation analysis approach [44]. The encode, delay and probe stage from each condition and every trial was modeled with its own distinct regressor within the GLM, although only the encode period activity was analyzed below. The average value was extracted for each VAC ROI for each trial and these values were then correlated voxel-wise across the entire brain to find regions with co-varying activity across trials with the VAC-ROI. The whole-brain r value maps for each participant underwent a Fisher's r to z transformation and the z-values were then normalized to the MNI-template and Gaussian smoothed (5 mm FWHM) for group level analysis. Group contrast maps were created by permuting across the condition grouping term and averaging across the group using 10000 rounds of permutation [53]. Data were corrected for multiple comparisons by thresholding the p-values at 0.05 and permuting across the expected cluster distribution to find the expected cluster size for $p = 0.05$. Clusters smaller than this value were removed from the analysis.

3.6.9 Whole-Brain Neural-Functional Connectivity Correlations

Correlations between each participant's index of suppression (encode period values for the PPA: the difference between the FM-O and PV-O conditions) and the degree of functional connectivity between the PPA and every other voxel were performed on MNI-normalized images, thresholded at $p < 0.05$ and corrected for multiple comparisons using the permutation method described in the Network Analysis section above.

3.6.10 Comparative Statistics

ANOVA's were utilized throughout analysis. Post-hoc two-tailed t-tests were corrected for multiple comparisons using Tukey-Kramer's method. One-tailed t-test were used when supported by the hypothesis (i.e. *condition 1* > *condition 2*) and were reported within the text.

Chapter 4

Conclusions

The results described here strongly support our hypothesis that age-related neuro-structural and functional changes underlie cognitive decline in healthy, older adults. In the Chapter 2, we found that there are separate enhancement and suppression networks, the frontal-parietal and default networks, respectively, and that the degree of VAC-default network engagement was predictive of neural suppression for the PPA. In Chapter 3, we replicated the age-related selective suppression deficit in which older adults show a decreased ability to ignore task-irrelevant information and that the degree of their suppression deficit was predictive of their performance [3]. Consistent with this age-related selective suppression deficit, we also found that older participants had reduced neuro-functionality of their suppression/default network and that older adults who were best able to deactivate their default network, were best able to maintain neural suppression and performance. Most importantly, however, we discovered that gray-matter atrophy within in the mPFC (a node of the suppression/default network in healthy, young controls) is predictive of older participants' ability to suppress task-irrelevant information and maintain working memory performance on a selective attention, working memory task. Taken together, these results support our hypothesis that age-related neuro-structural changes underlie neuro-functional changes that themselves underlie the effects of

cognitive aging.

In Chapter 2, we discovered that the goal-driven, or top-down, process of enhancement was associated with the frontal-parietal network while the process of suppression was associated with the default network. Unsurprisingly, the frontal-parietal network has previously been described as distal brain-regions that act in concert to direct attention towards external goals [35]. In this case, the frontal-parietal network may represent a direct source of attention-modulation of VAC regions. The default network result was, however, unexpected but also not surprising given what is known about the default network. Rather than describing the default network as regions that are active during internal monitoring states (such as prospective/retrospective memory and mind wandering [28, 31]), it is more useful in this case to consider them as regions that must be suppressed during an attentionally demanding task. Since suppression of these internal distractors is required for successful task-performance, it is computationally advisable to link these internal distractors with external distractors (as in task-irrelevant stimuli) and simply suppress both internal and external distractors simultaneously.

The argument may be made however, that this link between default network and suppression is purely correlative; since the default network must be deactivated for successful working memory performance, our measure of the suppression network may merely be reflective of the cognitive vigilance of the participants. Fortunately, we may directly refute this possibility within our data. It was only in the case where task-irrelevant information was present in the stimuli that we found a coupling between task-irrelevant VAC regions and the default network. If our suppression network was just a reflection of cognitive state as measured via default network deactivation, we would have expected to find task-irrelevant regions covary in time with the default network across all conditions (that is, during trials with high cognitive vigilance, there would be suppression of the default network and suppression of the irrelevant VAC), not only the ones containing task-irrelevant in-

formation. Interestingly, we found that default network deactivation was predictive of trial-by-trial performance supporting the hypothesis that " ... [both] inhibiting irrelevant information and being engaged in the task are necessary for the adequate performance of a WM task." [49] and that successful suppression of task-irrelevant information may drive performance [14].

In Chapter 3, we duplicated the age-related selective suppression deficit [3] showing that older adults did not suppress task-irrelevant information and that those who showed the least suppression, showed the worse performance. There was also a corresponding decrease in older adults' suppression network consistent with both their inability to suppress and reductions in default network functionality [32]. In older adults who demonstrated the greatest task-induced deactivation of their default network, there was greatest maintenance of both suppression and performance, further reinforcing the role of the default network in suppression.

Most interestingly, however, was that we were able to link age-related alterations in neuro-structural integrity with both maintenance of suppression and performance in older adults. We found that gray-matter atrophy in the mPFC was predictive of neural and cognitive decline. Those adults with the greatest gray-matter loss within the mPFC were those adults that demonstrated the lowest levels of both suppression and greatest susceptibility to distraction. Consistent with the role of the default network in suppression, the mPFC is actually a primary node of the default network and suppression network yet was no longer functionally coupled in healthy older adults and is one of the primary regions of default network dysfunction in healthy, older adults [1, 33]. These results strongly implicate the mPFC as a key attentional locus where local disruptions manifest themselves with global disruptions of neural and cognitive function.

The above experiments have demonstrated two major findings: 1) that there are separate, distinct, and dissociable neural networks associated with the top-down processes of enhancement and suppression and 2) that age-related alterations in

the suppression network may be driven by underlying neuro-structural changes and this age-related dysfunction is one of the primary driving forces behind the neuro-functional and cognitive effects of healthy, normal aging. Interestingly, these results demonstrate that changes in specific brain regions can have pronounced consequences in distal regions, supporting our methodology of recording whole-brain neural data and investigating large-scale network changes. Taken together, we have presented compelling evidence that age-related loss of specific brain regions may globally affect neural function and, as a result, may be one of the principal driving forces behind cognitive aging.

Appendices

Appendix A

Enhancement Network Changes in Healthy, Older Adults

A.1 Introduction

The previous two chapters have demonstrated that 1) there are separate whole-brain networks associated with enhancement and suppression, the frontal-parietal network and the default network, respectively (chapter 2) and 2) that the suppression network and default network are degraded in older adults consistent with the observed age-related selective suppression deficit and the effects of cognitive aging. However, there exist age-related functional network changes unrelated to the process of suppression that have not been addressed above. As shown below, there is also an age-related alteration in the functionally defined enhancement network in older adults, yet there is no observable age-related change in the process of enhancement within older adults. The notion that there is maintenance of enhancement and alterations in the enhancement network is strongly suggestive that these observed changes may be manifestations of age-related compensatory mechanisms. If the results below are indeed related to compensatory changes, they suggest that

the brains of older adults undergo functional reorganizations to maintain enhancement. Since the observed changes are consistent with the loss of specific brain regions from the suppression network (specifically the medial prefrontal cortex, mPFC), the possibility remains that the process of enhancement is maintained at the loss of the process of suppression.

Age-related activity and network changes have previously been described in older adults. Older adults show an age-related increases in bilateral activations compared to younger, unilateral activations (hemispherical asymmetry reduction in older adults, HAROLD [61]) as well as increased brain activations in regions that are unrelated to task activity in younger adults in the face of increasing task difficulty (compensation-related utilization of neural circuits hypothesis, CRUNCH [9]). It is hypothesized that these age related reorganizations are a compensatory response to "...declining neural structures and functions" (scaffolding theory of aging and cognition, STAC [8]) and that, in older adults who have diminished neural resources, these changes in activations represent a compensatory mechanism to maintain cognitive function.

Given that there were no observed age-related compensatory changes within the suppression network (Chapter 3), it is tempting to suggest that this is not occurring within the previous experiment. However, since there was an age-related failure to suppress, it is not surprising that there were no suppression related compensatory changes since there was a loss of suppression rather than maintenance of it in the face of diminished resources. When the enhancement network is analyzed, there are significant age-related changes that are correlated with maintenance of both enhancement and behavioral performance in the face of distraction, suggesting that there are compensatory mechanisms that work to maintain enhancement in healthy, older adults. Since the mPFC is both involved in suppression in healthy, younger controls and now associated with enhancement in older adults, one explanation of the age-related selective suppression deficit could be that older adults

exhibit compensatory mechanisms that maintain enhancement at the cost of suppression.

A.2 Results and Discussion

To investigate if there were age-related changes to the enhancement network, a contrast was created for the enhancement network for younger vs. older participants (i.e. whole-brain and PPA functional connectivity contrast between young and old participants for SM-O > PV-O, see Materials and Methods, Chapter 2). The younger participants showed that the canonical frontal-parietal network is associated with enhancement (Figure A.1A and chapter 2) while the older participants showed a similar pattern of frontal-parietal connectivity in addition to a region within the mPFC (Figure A.1B). Interestingly, this mPFC region was previously associated with suppression in younger participants (Chapter 2) but was no longer associated with suppression in older adults (Chapter 3). The mPFC was significantly more connected during enhancement for the older participants compared to the younger participants (Figure A.1C).

This result suggests that older adults utilize the mPFC as part of the enhancement network but does not signify if this is a beneficial effect. For example, it could be the case that incorporation of the mPFC into the enhancement network is causal/predictive of cognitive decline and that those older adults who utilize the mPFC as a node within the enhancement network are those adults who have the most pronounced suppression deficit and associated performance reductions. Or it could be the case that those older participants who utilize the mPFC as part of the enhancement network are those that maintain performance as compared to healthy younger controls. Unfortunately, there is no significant correlation between either VAC modulation or behavioral performance and mPFC recruitment so any link between the mPFC and neural compensation in older adults is purely

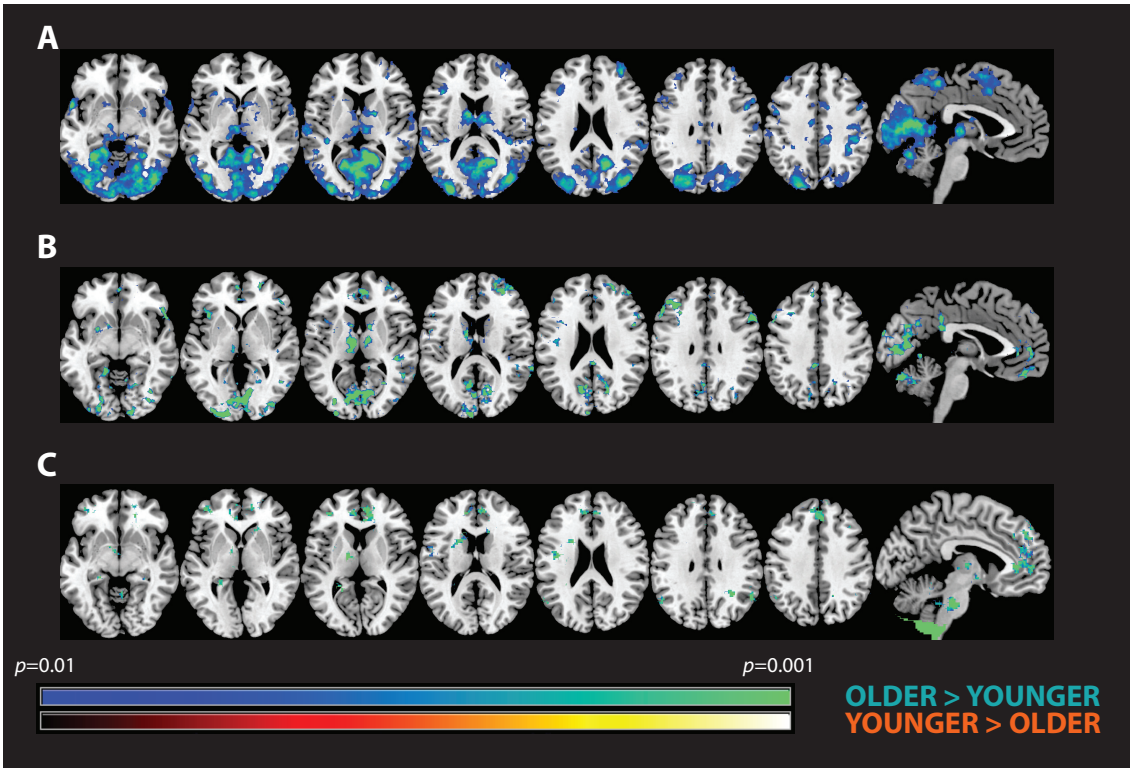

Figure A.1: *Younger vs. Older Enhancement Network.* A) Younger participants' enhancement network (PPA connectivity: SM-O > PV-O). B) Older participants' enhancement network. C) Comparison between younger and older participants. All images were thresholded at $p < 0.01$ and cluster corrected as previously described.

speculative.

As the brain ages, it is theorized that there is reduced processing capacity in any given unit of cortex [8]. In tasks with low cognitive demands, there exists "spare" processing capacity whereby regions that are not normally active in healthy, young controls now show task-related activity in older participants [61]. This, however, does not suggest that these compensatory changes should allow older participants to maintain cognitive performance at the level of healthy, young controls. In fact, since these compensatory regions have not been "honed" since birth to accomplish a specific computation, these regions are inherently inefficient [8]. However, when this "spare" capacity is exceeded by task-demands and the brain is unable to assemble an effective compensatory reaction, behavioral performance will suffer and drop off precipitously [8]. If the older participants in the above study lacked sufficient

processing resources to maintain both enhancement and suppression, it is possible that participants' brains may compensate in such a way to maintain enhancement at the cost of suppression.

Appendix B

rTMS Affects on Top-Down Modulation and Attentional Networks

B.1 Introduction

The previous section indicated that we may be observing lifespan-related neural compensation in older adults and that perhaps those who show this compensation also show the greatest maintenance of performance in the face of distraction. To test the observation that age-related perturbations of neural processing capacity result in compensatory changes that preferentially maintain enhancement at the cost of suppression, we utilized repetitive-pulse transcranial magnetic stimulation (rTMS) to selectively perturb [75] a node within the enhancement network to see if we can 1) elicit a behavioral effect of perturbing these network, 2) affect our measure of top-down modulation, and 3) investigate if there are compensatory network changes that account for neural and behavioral changes.

Unfortunately, while we were unable to effect behavior at the group level, there are

several neural effects of rTMS described below that are suggestive of rapidly-acting compensatory mechanisms. These include an rTMS induced selective suppression deficit and activity and network changes consistent with the notion of neural compensation.

B.2 Materials and Methods

22 younger participants (18-33 years old; mean, 24.2) were enrolled in the two-part study, however, data were collected for both sessions for only 19 participants. The first visit consisted of an fMRI session using the exact methods described previously (Chapter 2). After the first session, functional connectivity maps were derived in native-space for each participant. Using the map of L-PPA connectivity during the SM-O condition (remember scenes, ignore faces), the enhancement network was defined for each participant. Each participant's T1 anatomical image and PPA-enhancement network map were loaded into Brainsight Stereotaxic Software (Rogue Research, Montreal, Canada). Each individual's right Inferior Frontal Junction (IFJ) was identified by finding the region of maximal functional connectivity to the PPA during enhancement while constraining identification by anatomical features. The right IFJ was chosen because it shows significant functional connectivity to both the PPA and FFA during enhancement but not suppression.

For the second session, participants were met in the stereotaxic equipment room and their IFJ location was marked on their scalp using a permanent marker. Participants were then transported to the fMRI site for the remainder of the experiment. For the second session, a similar paradigm was used as in the previous two chapters except that the conditions FM and SM (remember faces, no-overlap and remember scenes, no-overlap, respectively) were omitted from the second session. In addition, blocks were expanded to 30 trials each (Fig. B.1). There were a total of three trial block types: FM-O (remember faces, overlap), PV-O (passive view, overlap), and

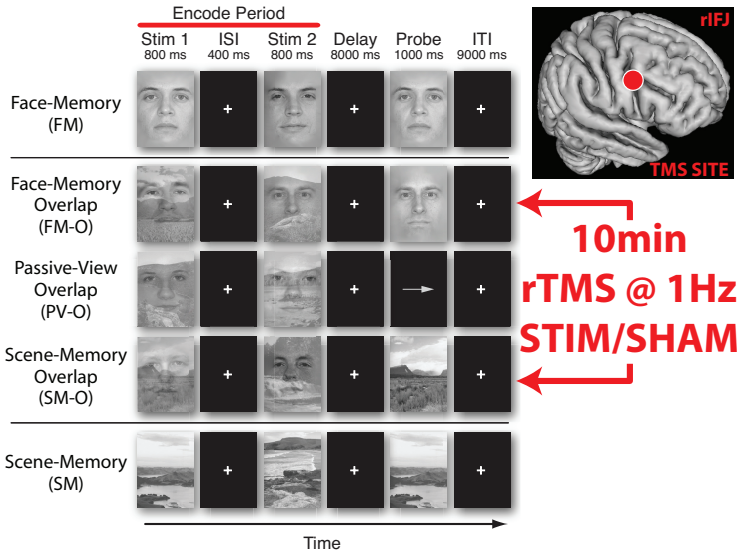

Figure B.1: *rTMS Task.* For Session 1, all conditions were run as described in Chapter 2. For Session 2, only the three overlapped conditions were run (SM-O, PV-O, and FM-O) with both STIM and SHAM rTMS at the IFJ (see insert for approximate location).

SM-O (remember scenes, overlap). For both the FM-O and SM-O conditions, there were two additional conditions: STIM and SHAM. STIM signifies 10 minutes of 1Hz rTMS at 70% maximum stimulator output over the right IFJ site while SHAM was 10 minutes of 1Hz rTMS sham stimulation over the same site (coil was held 90° to scalp). A Magstim Standard Rapid TMS Unit (Jali Medical Inc) was used to generate pulses with a 70 mm figure-of-eight induction coil. The magnetic stimulus had a biphasic waveform with a pulse width of about 300 μsec.

All conditions were presented pseudo-randomly for each participant and participants were not told whether they were receiving SHAM or STIM. After each rTMS application, participants were quickly moved into the scanner bore and an auto-align/shimming procedure was initiated to minimize across-block effects. Average time from final TMS pulse to acquisition of first fMRI volume was 2 minutes 31.9 seconds ($\pm$6.5 seconds). All data were analyzed offline as described in previous chapters.

B.3 Results and Discussion

To investigate if there was a group-level effect of rTMS, both working memory accuracy (WM) and response time (RT) data was compared for the STIM and SHAM conditions (Fig. B.2). Unfortunately, no main-effect was observed for rTMS type and results were consistent with previous findings across all trial-types (Chapter 1). However, since part of the working hypothesis was that the brain might display rapid-onset compensatory mechanisms, there may be changes within the attentional networks that compensate for the disruption of the IFJ.

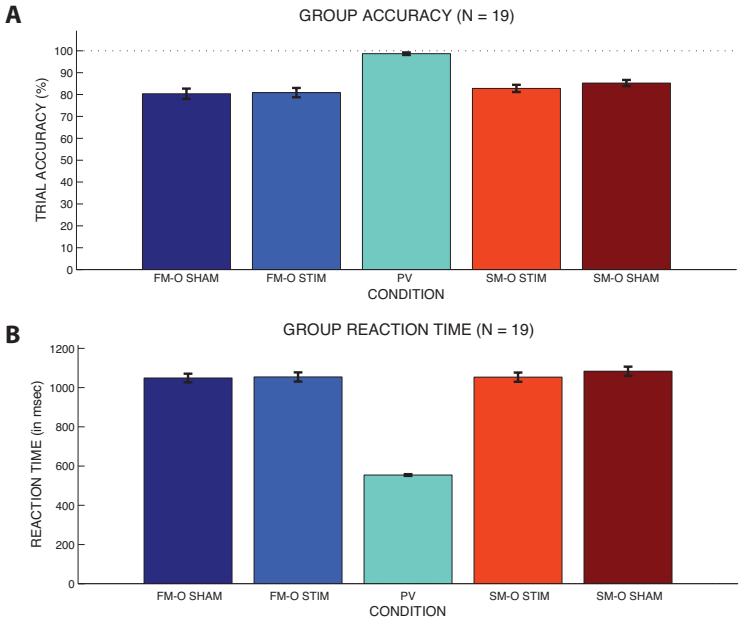

Figure B.2: *Behavioral Performance.* There was no rTMS effect (STIM vs. SHAM) for either working memory accuracy (A) or response time (B).

We next looked at PPA activity during the encode period to see if we had a neural effect of rTMS on top-down modulation (Fig. B.3). Surprisingly, PPA activity was affected during suppression but not enhancement even though the rTMS target (IFJ) was chosen because of its role in enhancement rather than suppression. This result is suggestive of one potential origin of the age-related selective suppression deficit: that there is a selective maintenance of enhancement at the cost of suppression due to declining neural resources. In this case, even though the enhancement

network was perturbed using rTMS, we find the neural effects manifest themselves via suppression. Perhaps neural resources destined for suppression-related processing are instead co-opted into the enhancement network to maintain functional levels of enhancement at the cost of suppression. We next looked at rTMS related activity changes across the whole-brain to probe for neural signatures of compensation.

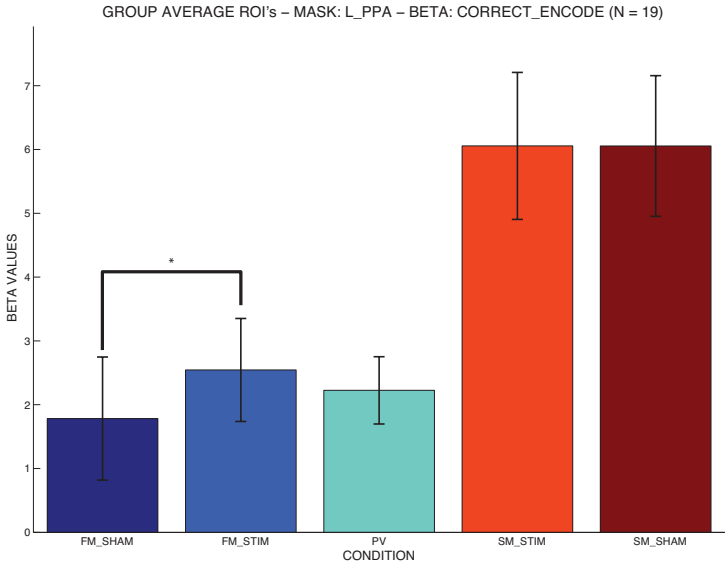

Figure B.3: *PPA ROI Results.* The only significant effect of rTMS was shown for FM-STIM > FM-SHAM, $p < 0.05$.

When we collapsed across instructions to directly compare STIM vs. SHAM, we found two prominent frontal regions that are significantly more active in the STIM conditions vs. SHAM: the right middle frontal gyrus (rMFG) and a non-surface rIFJ region (Fig. B.4). Interestingly, this rMFG region was one of two potential rTMS sites that were differentially and functionally connected with the PPA during enhancement but not suppression. This result implies that when there is perturbation to a node within this enhancement network, other regions may compensate for this disruption by increasing their activity. We then performed an across participant correlation between the magnitude of rMFG activity and performance in both the STIM and SHAM conditions (using FM-O as this was the condition when suppression of the PPA is occurring). We found that, during the STIM condition,

increased rMFG activity was correlated with increased RT performance (Fig B.5: $r = -0.51$, $p < 0.02$)[1] but not during the SHAM condition, suggesting that those participants who increase rMFG activity in response to perturbation of another node within the enhancement network, perform the best.

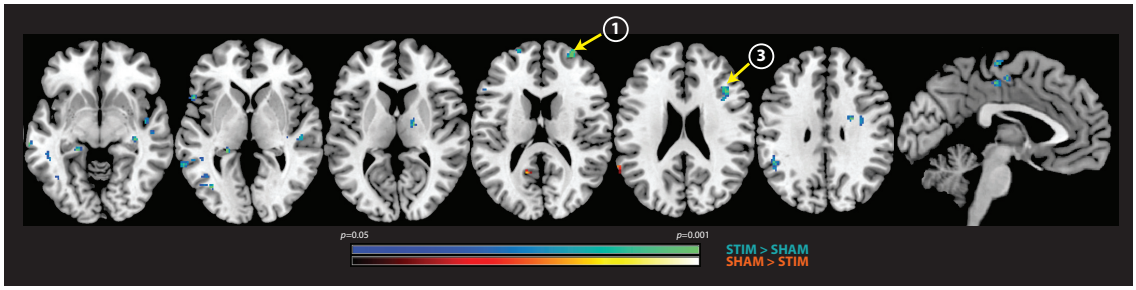

Figure B.4: *Univariate Activity Effects of rTMS.* Both the right middle frontal gyrus (1 – rMFG) and a deep right inferior frontal junction (2 – IFJ) showed increased activity in response to rTMS. Images were thresholded at $p < 0.05$ and cluster corrected as described previously. Same numbered labels as in Figure 2.4.

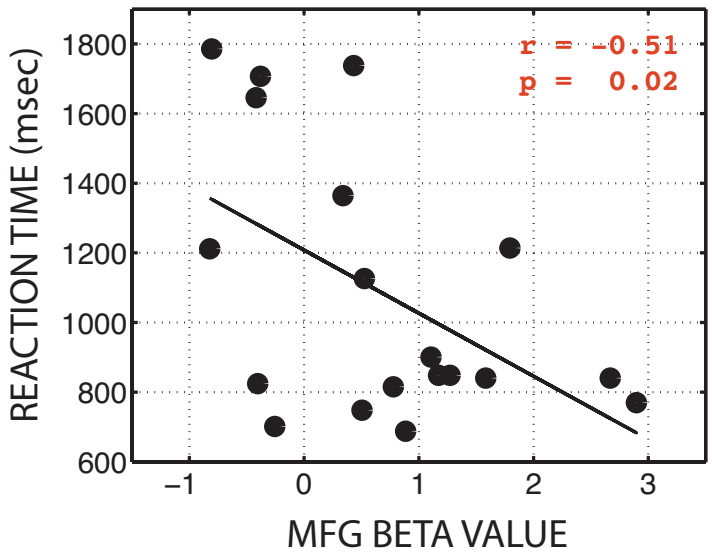

Figure B.5: *RT-MFG Activity Correlation.* Correlation between RT in the FM-STIM condition and MFG activity during FM-STIM.

To investigate if there were network changes associated with rTMS, we contrasted both the enhancement and suppression network maps for STIM and SHAM. For the

[1]Interestingly, during the SHAM condition, increased rMFG activity was correlated with decreased WM accuracy ($r = -0.54$, $p < 0.017$) but as this was using a different behavioral measure (RT), it is not statistically kosher to compare between the two.

enhancement network, the mPFC was significantly more correlated with the PPA during STIM than SHAM (Fig. B.6A) but not for the suppression network (Fig. B.6B). These results are intriguing since this is that same pattern of connectivity as found in healthy, older adults where mPFC: enhancement > suppression. In the case of older adults, there are across brain perturbations in structure/function that have accrued over their entire lifespan while in younger rTMS participants, this perturbation is localized and recent in origin.

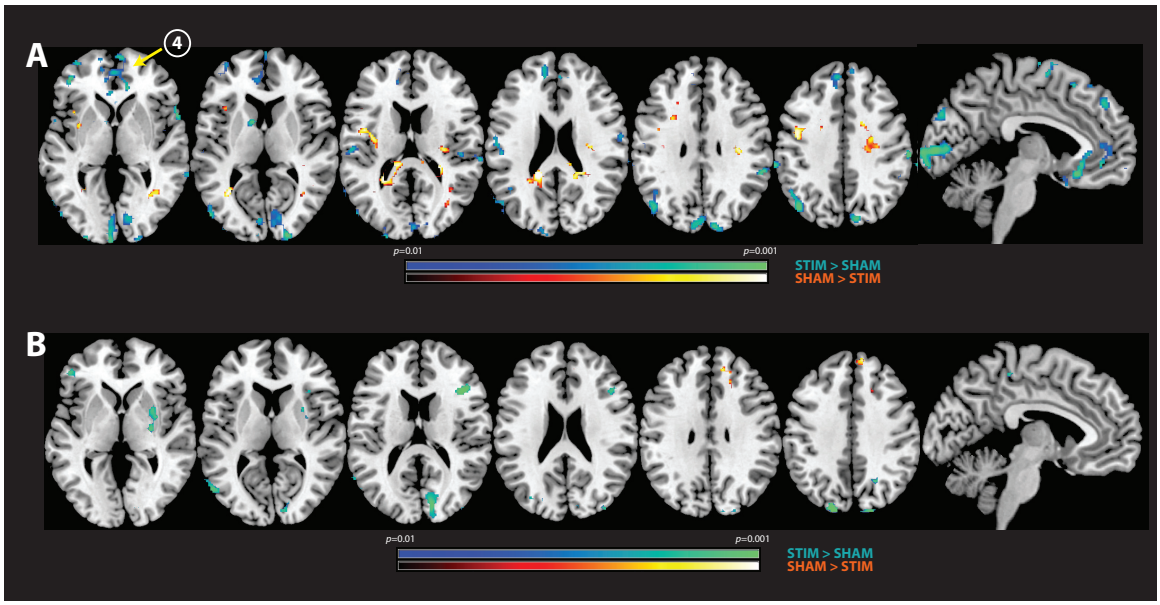

Figure B.6: *rTMS Effects on Attentional Networks.* A) The mPFC shows increased connectivity with the PPA during enhancement for STIM vs. SHAM. B) There is no mPFC connectivity statistically different for STIM vs. SHAM in the suppression network. Same numbered labels as in Figure 2.4.

In addition, as shown by an across participant whole-brain correlation, those participants who showed greatest recruitment of the mPFC into their enhancement network, were the same participants who showed the greatest total PPA modulation (Fig. B.7) suggesting that this recruitment of the mPFC into the enhancement network serves the purpose of maintaining the required degree of top-down modulation for successful performance. These putative compensatory changes may help to explain the lack of behavioral finding of rTMS. If younger participants have "spare" processing capacity compared to older adults, then the younger participants should

show a decreased sensitivity to perturbation of neural networks and should be able to demonstrate successful neural compensation to maintain performance. If a similar experiment was performed in healthy, older participants, it is expected that they would be significantly impacted by rTMS (compared to younger participants) due to decreased neural scaffolding reserves.

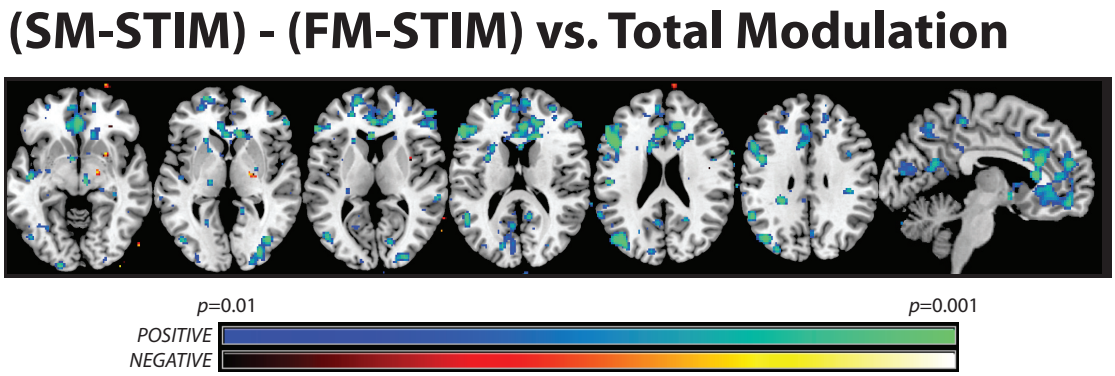

Figure B.7: *rTMS Effects on PPA Connectivity.* Correlation between PPA connectivity Enhancement/Suppression during STIM with total PPA modulation (SM-STIM - SM-SHAM). Participants with greater mPFC during enhancement showed greater total modulation. Images displayed at p¡0.01 and cluster corrected as previously described.

Literature Cited

[1] Andrews-Hanna, J. R. *et al.* Disruption of large-scale brain systems in advanced aging. *Neuron* **56**, 924–35 (2007). URL http://www.ncbi.nlm.nih.gov/entrez/query.fcgi?cmd=Retrieve&db=PubMed&dopt=Citation&list_uids=18054866%20.

[2] Greenwood, P. The frontal aging hypothesis evaluated. *J Int Neuropsychol Soc* **6**, 705–26 (2000). URL http://www.ncbi.nlm.nih.gov/entrez/query.fcgi?cmd=Retrieve&db=PubMed&dopt=Citation&list_uids=11011517%20.

[3] Gazzaley, A., Cooney, J., Rissman, J. & D'Esposito, M. Top-down suppression deficit underlies working memory impairment in normal aging. *Nat Neurosci* **8**, 1298–300 (2005). URL http://www.ncbi.nlm.nih.gov/entrez/query.fcgi?cmd=Retrieve&db=PubMed&dopt=Citation&list_uids=16158065%20.

[4] Raz, N. *et al.* Selective aging of the human cerebral cortex observed in vivo: differential vulnerability of the prefrontal gray matter. *Cereb Cortex* **7**, 268–82 (1997). URL http://www.ncbi.nlm.nih.gov/entrez/query.fcgi?cmd=Retrieve&db=PubMed&dopt=Citation&list_uids=9143446%20.

[5] Grady, C. L. *et al.* Age-related changes in cortical blood flow activation during visual processing of faces and location. *J Neurosci* **14**, 1450–62 (1994). URL http://www.ncbi.nlm.nih.gov/entrez/query.fcgi?cmd=Retrieve&db=PubMed&dopt=Citation&list_uids=8126548%20.

[6] Thomsen, T. *et al.* Brain localization of attentional control in different age groups by combining functional and structural mri. *NeuroImage* **22**, 912–9 (2004). URL http://www.ncbi.nlm.nih.gov/entrez/query.fcgi?cmd=Retrieve&db=PubMed&dopt=Citation&list_uids=15193622%20.

[7] Gazzaley, A. & D'Esposito, M. Top-down modulation and normal aging. *Ann N Y Acad Sci* **1097**, 67–83 (2007). URL http://www.ncbi.nlm.nih.gov/entrez/query.fcgi?cmd=Retrieve&db=PubMed&dopt=Citation&list_uids=17413013%20. Journal Article Review United States.

[8] Park, D. C. & Reuter-Lorenz, P. A. The adaptive brain: aging and neurocognitive scaffolding. *Annual review of psychology* **60**, 173–96 (2009). URL http://arjournals.annualreviews.org/doi/abs/10.1146/annurev.psych.59.103006.093656?url_ver=Z39.88-2003&rfr_id=ori:rid:crossref.org&rfr_dat=cr_pub%253dncbi.nlm.nih.gov.

[9] Schneider-Garces, N. J. *et al.* Span, crunch, and beyond: Working memory capacity and the aging brain. *J Cogn Neurosci* **22**, 655–669 (2009). URL http://www.mitpressjournals.org/doi/abs/10.1162/jocn.2009.21230?url_ver=Z39.88-2003&rfr_id=ori:rid:crossref.org&rfr_dat=cr_pub%253dncbi.nlm.nih.gov.

[10] Moran, J. & Desimone, R. Selective attention gates visual processing in the extrastriate cortex. *Science* **229**, 782–4 (1985). URL http://www.ncbi.nlm.nih.gov/entrez/query.fcgi?cmd=Retrieve&db=PubMed&dopt=Citation&list_uids=4023713%20. Journal Article United states.

[11] Spitzer, H. & Richmond, B. Task difficulty: ignoring, attending to, and discriminating a visual stimulus yield progressively more activity in inferior temporal neurons. *Exp Brain Res* **83**, 340–8

(1991). URL http://www.ncbi.nlm.nih.gov/entrez/query.fcgi?cmd=Retrieve&db=PubMed&dopt=Citation&list_uids=2022243%20.

[12] Gazzaley, A., Cooney, J., McEvoy, K., Knight, R. T. & D'Esposito, M. Top-down enhancement and suppression of the magnitude and speed of neural activity. *J Cogn Neurosci* **17**, 507–17 (2005). URL http://www.ncbi.nlm.nih.gov/entrez/query.fcgi?cmd=Retrieve&db=PubMed&dopt=Citation&list_uids=15814009%20.

[13] Rutman, A. M., Clapp, W. C., Chadick, J. & Gazzaley, A. Early top-down control of visual processing predicts working memory performance. *J Cogn Neurosci* **22**, 1224–1234 (2009). URL http://www.mitpressjournals.org/doi/abs/10.1162/jocn.2009.21257?url_ver=Z39.88-2003&rfr_id=ori:rid:crossref.org&rfr_dat=cr_pub%253dncbi.nlm.nih.gov.

[14] Zanto, T. P. & Gazzaley, A. Neural suppression of irrelevant information underlies optimal working memory performance. *J Neurosci* **29**, 3059–66 (2009). URL http://www.jneurosci.org/cgi/content/full/29/10/3059.

[15] Gazzaley, A. *et al.* Functional interactions between prefrontal and visual association cortex contribute to top-down modulation of visual processing. *Cereb Cortex* **17 Suppl 1**, i125–35 (2007). URL http://www.ncbi.nlm.nih.gov/entrez/query.fcgi?cmd=Retrieve&db=PubMed&dopt=Citation&list_uids=17725995%20.

[16] Cavada, C. & Goldman-Rakic, P. Posterior parietal cortex in rhesus monkey: Ii. evidence for segregated corticocortical networks linking sensory and limbic areas with the frontal lobe. *J Comp Neurol* **287**, 422–45 (1989). URL http://www.ncbi.nlm.nih.gov/entrez/query.fcgi?cmd=Retrieve&db=PubMed&dopt=Citation&list_uids=2477406%20.

[17] Morris, R., Pandya, D. N. & Petrides, M. Fiber system linking the mid-dorsolateral frontal cortex with the retrosplenial/presubicular region in the

rhesus monkey. *J Comp Neurol* **407**, 183–92 (1999).

[18] Petrides, M. & Pandya, D. N. Efferent association pathways from the rostral prefrontal cortex in the macaque monkey. *J Neurosci* **27**, 11573–86 (2007). URL http://www.jneurosci.org/cgi/content/full/27/43/11573.

[19] Petrides, M. & Pandya, D. N. Projections to the frontal cortex from the posterior parietal region in the rhesus monkey. *J Comp Neurol* **228**, 105–16 (1984). URL http://www.ncbi.nlm.nih.gov/sites/entrez?Db=pubmed&Cmd=Retrieve&list_uids=6480903&dopt=abstractplus.

[20] Barcelo, F., Suwazono, S. & Knight, R. T. Prefrontal modulation of visual processing in humans. *Nat Neurosci* **3**, 399–403 (2000). URL http://www.ncbi.nlm.nih.gov/entrez/query.fcgi?cmd=Retrieve&db=PubMed&dopt=Citation&list_uids=10725931%20.

[21] Fuster, J., Bauer, R. & Jervey, J. Functional interactions between inferotemporal and prefrontal cortex in a cognitive task. *Brain Res* **330**, 299–307 (1985). URL http://www.ncbi.nlm.nih.gov/entrez/query.fcgi?cmd=Retrieve&db=PubMed&dopt=Citation&list_uids=3986545%20. Journal Article Netherlands.

[22] Fuster, J. Network memory. *Trends Neurosci* **20**, 451–9 (1997). URL http://www.ncbi.nlm.nih.gov/entrez/query.fcgi?cmd=Retrieve&db=PubMed&dopt=Citation&list_uids=9347612%20. Journal Article Review England.

[23] Fuster, J. M. & Alexander, G. E. Delayed response deficit by cryogenic depression of frontal cortex. *Brain Res* **20**, 85–90 (1970).

[24] Tomita, H., Ohbayashi, M., Nakahara, K., Hasegawa, I. & Miyashita, Y. Top-down signal from prefrontal cortex in executive control of memory re-

trieval. *Nature* **401**, 699–703 (1999). URL http://www.nature.com/nature/journal/v401/n6754/full/401699a0.html.

[25] Miller, B., Verstynen, T., Johnson, M. & D'Esposito, M. Prefrontal and parietal contributions to refreshing: an rtms study. *NeuroImage* **39**, 436–40 (2008). URL http://www.ncbi.nlm.nih.gov/entrez/query.fcgi?cmd=Retrieve&db=PubMed&dopt=Citation&list_uids=17936014%20.

[26] Corbetta, M., Patel, G. & Shulman, G. L. The reorienting system of the human brain: from environment to theory of mind. *Neuron* **58**, 306–24 (2008). URL http://linkinghub.elsevier.com/retrieve/pii/S0896-6273(08)00369-3.

[27] Fox, M. D. *et al.* The human brain is intrinsically organized into dynamic, anticorrelated functional networks. *Proc Nat Acad Sci USA* **102**, 9673–8 (2005).

[28] Buckner, R. L., Andrews-Hanna, J. R. & Schacter, D. L. The brain's default network: anatomy, function, and relevance to disease. *Ann N Y Acad Sci* **1124**, 1–38 (2008).

[29] Raichle, M. E. *et al.* A default mode of brain function. *Proc Nat Acad Sci USA* **98**, 676–82 (2001). URL http://www.pnas.org/content/98/2/676.long.

[30] Buckner, R. L. & Carroll, D. C. Self-projection and the brain. *Trends Cogn Sci* **11**, 49–57 (2007). URL http://www.sciencedirect.com/science?_ob=ArticleURL&_udi=B6VH9-4MMP640-1&_user=4430&_rdoc=1&_fmt=&_orig=search&_sort=d&_docanchor=&view=c&_acct=C000059594&_version=1&_urlVersion=0&_userid=4430&md5=9bc3e189b3c64e12cf7742c904720cd5.

[31] Mason, M. F. *et al.* Wandering minds: the default network and stimulus-independent thought. *Science* **315**, 393–5 (2007).

[32] Persson, J., Lustig, C., Nelson, J. K. & Reuter-Lorenz, P. A. Age differences in deactivation: a link to cognitive control? *J Cogn Neurosci* **19**, 1021–32

(2007).

[33] Grady, C. L. *et al.* A multivariate analysis of age-related differences in default mode and task-positive networks across multiple cognitive domains. *Cereb Cortex* **20**, 1432–1447 (2010). URL http://cercor.oxfordjournals.org/cgi/content/full/bhp207v1.

[34] Lustig, C. *et al.* Functional deactivations: change with age and dementia of the alzheimer type. *Proc Nat Acad Sci USA* **100**, 14504–9 (2003).

[35] Corbetta, M. Frontoparietal cortical networks for directing attention and the eye to visual locations: identical, independent, or overlapping neural systems? *Proc Nat Acad Sci USA* **95**, 831–8 (1998).

[36] Spitzer, H., Desimone, R. & Moran, J. Increased attention enhances both behavioral and neuronal performance. *Science* **240**, 338–40 (1988). URL http://www.ncbi.nlm.nih.gov/entrez/query.fcgi?cmd=Retrieve&db=PubMed&dopt=Citation&list_uids=3353728%20.

[37] Gazzaley, A. *et al.* Age-related top-down suppression deficit in the early stages of cortical visual memory processing. *Proc Nat Acad Sci USA* **105**, 13122–6 (2008). URL http://www.pnas.org/content/105/35/13122.

[38] Rissman, J., Gazzaley, A. & D'Esposito, M. The effect of non-visual working memory load on top-down modulation of visual processing. *Neuropsychologia* **47**, 1637–46 (2009).

[39] Kastner, S. & Ungerleider, L. G. Mechanisms of visual attention in the human cortex. *Annu Rev Neurosci* **23**, 315–41 (2000). URL http://www.ncbi.nlm.nih.gov/entrez/query.fcgi?cmd=Retrieve&db=PubMed&dopt=Citation&list_uids=10845067%20. Journal Article Review United states.

[40] Szczepanski, S. M., Konen, C. S. & Kastner, S. Mechanisms of spatial attention control in frontal and parietal cortex. *J Neurosci* **30**, 148–60 (2010).

[41] Weidner, R., Krummenacher, J., Reimann, B., Müller, H. J. & Fink, G. R. Sources of top-down control in visual search. *J Cogn Neurosci* **21**, 2100–13 (2009).

[42] Broyd, S. J. *et al.* Default-mode brain dysfunction in mental disorders: a systematic review. *Neurosci Biobehav Rev* **33**, 279–96 (2009). URL http://www.sciencedirect.com/science?_ob=ArticleURL&_udi=B6T0J-4TDC0DY-3&_user=4430&_rdoc=1&_fmt=&_orig=search&_sort=d&_docanchor=&view=c&_acct=C000059594&_version=1&_urlVersion=0&_userid=4430&md5=03c1cf2e43971d9f43a459ab560cfe27.

[43] Gazzaley, A., Rissman, J. & D'Esposito, M. Functional connectivity during working memory maintenance. *Cogn Affect Behav Neurosci* **4**, 580–99 (2004). URL http://www.ncbi.nlm.nih.gov/pubmed/15849899?dopt=abstract.

[44] Rissman, J., Gazzaley, A. & D'Esposito, M. Measuring functional connectivity during distinct stages of a cognitive task. *NeuroImage* **23**, 752–63 (2004). URL http://www.ncbi.nlm.nih.gov/entrez/query.fcgi?cmd=Retrieve&db=PubMed&dopt=Citation&list_uids=15488425%20.

[45] Capotosto, P., Babiloni, C., Romani, G. L. & Corbetta, M. Frontoparietal cortex controls spatial attention through modulation of anticipatory alpha rhythms. *J Neurosci* **29**, 5863–72 (2009).

[46] Grady, C. L., Springer, M. V., Hongwanishkul, D., McIntosh, A. R. & Winocur, G. Age-related changes in brain activity across the adult lifespan. *J Cogn Neurosci* **18**, 227–41 (2006).

[47] Moore, T. & Armstrong, K. M. Selective gating of visual signals by microstimulation of frontal cortex. *Nature* **421**, 370–3 (2003).

[48] Celone, K. A. *et al.* Alterations in memory networks in mild cognitive impairment and alzheimer's disease: an independent component analysis. *J Neurosci* **26**, 10222–31 (2006). URL http://www.ncbi.nlm.nih.gov/entrez/query.fcgi?db=pubmed&cmd=Retrieve&dopt=AbstractPlus&list_uids=17021177.

[49] Scheeringa, R. *et al.* Trial-by-trial coupling between eeg and bold identifies networks related to alpha and theta eeg power increases during working memory maintenance. *NeuroImage* **44**, 1224–38 (2009).

[50] Gusnard, D. A., Akbudak, E., Shulman, G. L. & Raichle, M. E. Medial prefrontal cortex and self-referential mental activity: relation to a default mode of brain function. *Proc Nat Acad Sci USA* **98**, 4259–64 (2001).

[51] Persson, J., Welsh, K. M., Jonides, J. J. & Reuter-Lorenz, P. A. Cognitive fatigue of executive processes: interaction between interference resolution tasks. *Neuropsychologia* **45**, 1571–9 (2007). URL http://www.sciencedirect.com/science?_ob=ArticleURL&_udi=B6T0D-4MV1H8V-3&_user=4430&_coverDate=12%252F31%252F2007&_rdoc=1&_fmt=high&_orig=search&_sort=d&_docanchor=&view=c&_acct=C000059594&_version=1&_urlVersion=0&_userid=4430&md5=85e102b3458cf28ba9c01a0e6e29b681.

[52] Hedden, T. *et al.* Disruption of functional connectivity in clinically normal older adults harboring amyloid burden. *J Neurosci* **29**, 12686–94 (2009).

[53] Nichols, T. E. & Holmes, A. P. Nonparametric permutation tests for functional neuroimaging: a primer with examples. *Hum Brain Mapp* **15**, 1–25 (2002). URL http://www3.interscience.wiley.com/journal/86010644/abstract?CRETRY=1&SRETRY=0.

[54] Grady, C. L. Functional brain imaging and age-related changes in cognition. *Biol Psychol* **54**, 259–81 (2000). URL http://www.ncbi.nlm.nih.

gov/entrez/query.fcgi?cmd=Retrieve&db=PubMed&dopt=Citation&list_uids=11035226%20.

[55] Pasternak, T. & Greenlee, M. W. Working memory in primate sensory systems. *Nat Rev Neurosci* **6**, 97–107 (2005). URL http://www.ncbi.nlm.nih.gov/entrez/query.fcgi?cmd=Retrieve&db=PubMed&dopt=Citation&list_uids=15654324%20.

[56] D'Esposito, M., Postle, B. R. & Rypma, B. Prefrontal cortical contributions to working memory: evidence from event-related fmri studies. *Exp Brain Res* **133**, 3–11 (2000). URL http://www.ncbi.nlm.nih.gov/entrez/query.fcgi?cmd=Retrieve&db=PubMed&dopt=Citation&list_uids=10933205%20.

[57] Rajah, M., Ames, B. & D'Esposito, M. Prefrontal contributions to domain-general executive control processes during temporal context retrieval. *Neuropsychologia* **46**, 1088–103 (2008). URL http://www.ncbi.nlm.nih.gov/entrez/query.fcgi?cmd=Retrieve&db=PubMed&dopt=Citation&list_uids=18155254%20. Journal Article England.

[58] Cabeza, R. *et al.* Task-independent and task-specific age effects on brain activity during working memory, visual attention and episodic retrieval. *Cereb Cortex* **14**, 364–75 (2004). URL http://www.ncbi.nlm.nih.gov/entrez/query.fcgi?cmd=Retrieve&db=PubMed&dopt=Citation&list_uids=15028641%20.

[59] Faubert, J. & Bellefeuille, A. Aging effects on intra- and inter-attribute spatial frequency information for luminance, color, and working memory. *Vis Res* **42**, 369–78 (2002). URL http://www.ncbi.nlm.nih.gov/entrez/query.fcgi?cmd=Retrieve&db=PubMed&dopt=Citation&list_uids=11809488%20. Journal Article England.

[60] Grady, C. L. *et al.* Evidence from functional neuroimaging of a compensatory prefrontal network in alzheimer's disease. *J Neurosci* **23**, 986–93 (2003).

[61] Cabeza, R. Hemispheric asymmetry reduction in older adults: the harold model. *Psychol Aging* **17**, 85–100 (2002). URL http://psycnet.apa.org/index.cfm?fa=search.displayRecord&uid=2002-02028-007.

[62] Ashburner, J. & Friston, K. J. Unified segmentation. *NeuroImage* **26**, 839–51 (2005).

[63] Ashburner, J. & Friston, K. J. Voxel-based morphometry–the methods. *NeuroImage* **11**, 805–21 (2000).

[64] Rowe, G., Valderrama, S., Hasher, L. & Lenartowicz, A. Attentional disregulation: a benefit for implicit memory. *Psychol Aging* **21**, 826–30 (2006).

[65] Ryan, J. D., Leung, G., Turk-Browne, N. B. & Hasher, L. Assessment of age-related changes in inhibition and binding using eye movement monitoring. *Psychol Aging* **22**, 239–50 (2007).

[66] Park, D. C. *et al.* Aging reduces neural specialization in ventral visual cortex. *Proc Nat Acad Sci USA* **101**, 13091–5 (2004).

[67] Grady, C. L. *et al.* Age-related reductions in human recognition memory due to impaired encoding. *Science* **269**, 218–21 (1995). URL http://www.ncbi.nlm.nih.gov/entrez/query.fcgi?db=pubmed&cmd=Retrieve&dopt=AbstractPlus&list_uids=7618082.

[68] Folstein, M. F., Folstein, S. E. & McHugh, P. R. "mini-mental state". a practical method for grading the cognitive state of patients for the clinician. *Journal of psychiatric research* **12**, 189–98 (1975). URL http://www.sciencedirect.com/science?_ob=ArticleURL&_udi=B6T8T-460XFH9-7V&_user=4430&_rdoc=1&_fmt=&_orig=search&_sort=d&_docanchor=&view=c&_acct=C000059594&_version=1&_urlVersion=0&_userid=4430&md5=387e09acdb5bcddc647a87dac1928264.

[69] Osterrieth, P. Le test de copie d'une figure complexe; contribution à l'étude de la perception et de la mémoire. *Archives de psychologie* (1944). URL http://psycnet.apa.org/?fa=main.doiLanding&uid=1946-02126-001.

[70] Rey, A. L'examen psychologique dans les cas d'enchephalapathie traumatique. *Archives de psychologie* **28**, 286–340 (1941).

[71] Kanwisher, N., McDermott, J. & Chun, M. M. The fusiform face area: a module in human extrastriate cortex specialized for face perception. *J Neurosci* **17**, 4302–11 (1997). URL http://www.jneurosci.org/cgi/content/full/17/11/4302.

[72] Wechsler, D. *Wechsler Adult Intelligence Scale-Revised Manual* (The Psychological Corporation, New York, 1981).

[73] Bentin, S., Allison, T., Puce, A., Perez, E. & McCarthy, G. Electrophysiological studies of face perception in humans. *J Cogn Neurosci* (1996). URL http://doi.apa.org/?uid=1997-02599-006.

[74] Epstein, R. & Kanwisher, N. A cortical representation of the local visual environment. *Nature* **392**, 598–601 (1998). URL http://www.nature.com/nature/journal/v392/n6676/full/392598a0.html.

[75] Thut, G. & Pascual-Leone, A. A review of combined tms-eeg studies to characterize lasting effects of repetitive tms and assess their usefulness in cognitive and clinical neuroscience. *Brain Topogr* **22**, 219–32 (2010). URL http://www.springerlink.com/content/2t1331372r3m07xj/.

Publishing Agreement

It is the policy of the University to encourage the distribution of all theses, dissertations, and manuscripts. Copies of all UCSF theses, dissertations, and manuscripts will be routed to the library via the Graduate Division. The library will make all theses, dissertations, and manuscripts accessible to the public and will preserve these to the best of their abilities, in perpetuity.

Please sign the following statement:

I hereby grant permission to the Graduate Division of the University of California, San Francisco to release copies of my thesis, dissertation, or manuscript to the Campus Library to provide access and preservation, in whole or in part, in perpetuity.



Author

29 November 2010

Date